REGULATION OF MMP9 BY MEF2A AND STAT3 IN NEONATAL RAT VENTRICULAR CARDIOMYOCYTES

Gurnoor Kaur Brar

A thesis submitted to the Faculty of Graduate Studies
in partial fulfillment of the requirements for the degree of

MASTER OF SCIENCE

Graduate Program in Biology
York University
Toronto, Ontario

March 2023

ABSTRACT

The myocyte enhancer factor-2 (MEF2) transcription factor is critical for defining cardiac-specific gene expression programs that have fundamental roles in differentiation and development. This thesis explored the effects of a novel protein:protein interaction between the MEF2A and signal transducer and activator of transcription-3 (STAT3) on matrix metalloproteinase (MMP9) transcriptional regulation in neonatal rat ventricular cardiomyocytes (NRVMs). Immunoprecipitation experiments confirmed a robust interaction between endogenous MEF2A and STAT3 within the NRVMs. SiRNA-mediated gene silencing and pharmacological inhibition revealed that MMP9 promoter activity, mRNA, and protein expression are significantly enhanced upon STAT3 depletion/inhibition and there is a marginal decrease in MMP9 mRNA upon MEF2A depletion. The foundational work in this thesis sheds light on the MMP9 gene transcriptional regulation by both MEF2A and STAT3, having implications for cardiac physiology and pathology associated with MMP9.

ACKNOWLEDGEMENTS

Graduate school during COVID-19 has been an interesting experience, I would like to take this time to acknowledge the individuals who have contributed to my success.

My supervisor, Dr. John C. McDermott, who took me in as a transfer student and provided the most supportive environment a graduate student could hope for. My advisor, Dr. Terrance Kubiseski, who provided constructive feedback and valuable suggestions throughout this project. It was not easy to finish a new masters project in under a year, however, it was worth it. I would like to express my deepest gratitude to all the members of the McDermott lab, Amira Moustafa, Xiaodong Gao, and Amanvir Virdi from Dr. Tsushima's lab for always being available to answer my countless questions. A big thank you to Debra Reid for looking after my rats in the vivarium.

I am fortunate to have a group of amazing friends, who have been the best support system: Bharat, Katlin, Tracy, Saja, Manpreet, and Amanvir. My partner, Aniket, thank you for being my rock and helping me stay positive in difficult situations. Lastly, I am thankful to my parents, both sets of grandparents, and my younger siblings; Bakhshish and Japnaam; for without their constant love, support, patience, and encouragement, I would have never made it this far.

TABLE OF CONTENTS

LIST OF FIGURES

LIST OF TABLES

COPYRIGHT PERMISSIONS AND ACKNOWLEDGEMENTS

STATEMENT OF TECHNICAL CONTRIBUTIONS

Experiments and analyses were performed **by Gurnoor Kaur Brar (GKB)**, in addition to those clarified below, in terms of technical expertise and experimental contribution to this thesis. Figures, tables, and illustrations were made by **GKB**, unless referenced otherwise. I acknowledge the following individuals for their technical or experimental contributions to this thesis:

1. **Dr. John C. McDermott** – Dr. McDermott heavily assisted me with study concept, design, development of methodology, statistical analysis and troubleshooting multiple aspects of this project.

2. **Amira Moustafa** – Amira was responsible for developing the experimental design alongside Dr. McDermott. She assisted me with cardiomyocyte isolations, transfections, immunoprecipitation, drug dilution, luciferase reporter assay, plasmid preparations and data analysis. She also conducted all the siRNA transfections (N=3) in cardiomyocytes for the luciferase assay and western blot experiments (**Figures 9B, 11 and 12**).

3. **Dr. Tetsuaki Miyake** – Dr. Miyake contributed a technical suggestion to administer pharmacological inhibitors to evaluate the resultant effects on the protein of interest and luciferase reporter activity (**Figure 12**).

4. **Amanvir Virdi** – Amanvir (from the Tsushima Lab) assisted me with methodology pertaining to the RNA extractions, protein extraction post-RNA extraction, RT-qPCR primer design, primer optimization and $2^{-\Delta\Delta Ct}$ analysis (**Figure 14**).

5. **Xiaodong Gao (XD)** – XD assisted me with reverse transcription of total RNA to cDNA.

CONTRIBUTION TO SCIENTIFIC MANUSCRIPT

I contributed the following experimental data analyses and figures from this thesis to the following scientific manuscript, which has been **accepted for publication** in ***Cell Death & Disease*** (manuscript #CDDIS-22-2362R) as of **February 8th, 2023.**

Figures 11 and 12 in this thesis are referenced as **Figure 7** in the manuscript.

Manuscript Title: **The MEF2A Transcription Factor Interactome in Cardiomyocytes**

Manuscript Authors: Amira Moustafa[1,2,3], Sara Hashemi[4], **Gurnoor Brar[1,2,3]**, Jörg Grigull[5], Siemon H. S. Ng[4], Declan Williams[6], Gerold Schmitt-Ulms[6] and John C. McDermott[1,2,3*]

[1]Department of Biology, York University, Toronto, ON, M3J 1P3, Canada

[2]Muscle Health Research Centre (MHRC), York University, Toronto, ON, M3J 1P3, Canada

[3]Centre for Research in Biomolecular Interactions (CRBI), York University, Toronto, ON, M3J 1P3, Canada

[4]Analytical Sciences, Sanofi Pasteur, Toronto, ON M2R 3T4, Canada. Current affiliation: Notch Therapeutics, Toronto, ON, M5G 1M1, Canada

[5]Department of Mathematics and Statistics, York University, Toronto, Ontario, M3J1P3, Canada

[6]Tanz Centre for Research in Neurodegenerative Diseases and Departments of Medicine, Medical Biophysics and Laboratory Medicine and Pathobiology, University of Toronto, Toronto, ON M5S 3H2, Canada

LIST OF ABBREVIATIONS

ChIP	Chromatin Immunoprecipitation
CREB	cAMP Response Element-Binding Protein
DBD	DNA Binding Domain
DNA	Deoxyribonucleic Acid
ERK	Extracellular signal-regulated protein kinases
GATA4	GATA Binding Protein 4
HAT	Histone Acetyltransferases
HDAC	Histone Deacetylases
LogFC	Logarithmic fold change
MADS	MCM1, Agamous, Deficiens, SRF
MAPK	Mitogen-Activated Protein kinase
MCM1	Mini Chromosome Maintenance 1
MEF2	Myocyte Enhancer Factor 2
MMP9	Matrix Metallopeptidase 9
mRNA	Messenger Ribonucleic Acid
NRVM	Neonatal Rat Ventricular Cardiomyocytes
CSX/NKX2.5	NK2 Homeobox 5
NLS	Nuclear Localization Sequence
p38	Protein 38 MAPK
Pol II	RNA Polymerase II
RNA	Ribonucleic Acid
RNAi	RNA interference
RT-qPCR	Reverse Transcription Quantitative Polymerase Chain Reaction
siRNA	Short Interfering RNA or Silencing RNA
SRF	Serum Response Factor
STAT3	Signal Transducer and Activator of Transcription 3
TAD	Transcriptional Activation Domain
TF	Transcription Factor

1. INTRODUCTION

1.1 General Overview

The control and regulation of gene expression is a fundamental biological process for cell growth, division, development, migration, and differentiation. The interaction of regulatory proteins with specific DNA motifs allows for the regulation of gene expression. Transcription factors are proteins that have one or more DNA-binding domains, which allow sequence-specific binding to cis-regulatory DNA sequences located in the regulatory regions of a gene (Spitz & Furlong, 2012). Upon binding to DNA, and through specific protein–protein interactions, the transcription factors convey activation or repression signals to the basal transcriptional machinery that regulate the period, amplitude, and duration of gene expression transcription (Latchman, 1997).

The heart is one of the first recognisable organs to develop in the embryo (Gittenberger-De Groot, Bartelings, Deruiter, & Poelmann, 2005). Cardiac transcription factors are at the center of an evolutionary conserved regulatory network defining cardiac cell fate, myogenic differentiation, morphogenesis, and cardiac-specific gene expression encoding structural and regulatory proteins (Olson, 2006). The core mammalian cardiac DNA-binding transcription factor network of GATA binding protein 4 (GATA4), Myocyte Enhancer Factor 2 (MEF2), NK2 homeobox 5 (NKX2.5), and Serum Response Factor (SRF) play pivotal roles in the differentiation, maturation, and homeostasis of cardiomyocytes. These core transcription factors cross regulate and autoregulate their expression, and act combinatorically on target downstream genes (Kohli, Ahuja, & Rani, 2012)

Cardiomyocytes are terminally differentiated cells and lose their ability to proliferate postnatally. Therefore, little can be done to recover heart function following significant cardiac stress. Disruptions to the cardiac regulatory network and the signaling components result in various mutant phenotypes in mice, congenital heart defects, and the activation of compensatory cardiac hypertrophy mechanisms (Gittenberger-De Groot et al., 2005; Wales, Hashemi, Blais, & Mcdermott, 2014). Investigating target gene expression by cardiac transcription factors may identify promising targets for efficient treatment strategies that can stimulate or inhibit transcription of specific genes for a desired therapeutic effect (Kohli et al., 2012)

In this introduction, I will first provide a brief overview of eukaryotic gene transcription highlighting the involvement of transcription factors and cis-regulatory elements (**Section 1.2**). Next, I will discuss mammalian cardiac development (**Section 1.3**). After this, I provide an overview of research related to the MEF2 transcription factor, a key focus of the McDermott Lab. I will discuss how MEF2 regulates gene expression in cardiomyocytes (**Section 1.4**) by reviewing key interactions of MEF2A with other transcription factors, and important upstream signalling cascades responsible for MEF2 dependent gene regulation in cardiomyocytes (**Section 1.5 - 1.6**). The rationale for this thesis will be highlighted in **Section 1.7** and the experimental hypothesis for this thesis will be covered in **Section 1.8**. This thesis focuses on using molecular biology techniques to confirm the downstream effects of a potential MEF2A:STAT3 protein:protein interaction on MMP9 activity using neonatal rat primary cardiomyocytes as the model organism for investigating the effects of this interaction.

1.2 Transcription in Eukaryotes

1.2.1 Overview of RNA Polymerase II-mediated Transcription Initiation

The expression of protein coding genes requires the synthesis of messenger RNA (mRNA) in a process called transcription. Transcription involves the binding of transcription related proteins to DNA cis-regulatory sequences in a region that is usually upstream of the transcription start site. Eukaryotic cis-regulatory elements can include, in addition to the core promoter, multiple enhancer regions, silencer regions, and insulators (Haberle & Stark, 2018). Enhancers can be situated upstream or downstream of the gene core promoter and within introns (Levine & Tjian, 2003). Additionally, enhancers can begin the process of the recruitment of activator transcriptional factors that modify chromatin structure and increase accessibility of the gene region that will be transcribed by the RNA polymerase II (Pol II). The eukaryotic enhancer regions can contain multiple gene-specific transcription factor binding sites, through which various combinations of transcription factors are recruited to activate transcription (Spitz & Furlong, 2012).

In contrast, silencer regions function to repress transcription, while insulators act as barriers to block the functionality of both the enhancer and silencer regions (Kolovos, Knoch, Grosveld, Cook, & Papantonis, 2012; Petrykowska, Vockley, & Elnitski, 2008). Like enhancers, silencers provide binding sites for repressor transcriptional factors, suggesting that repressors are involved in gene silencing through the modification of the chromatin state or occluding activator transcriptional factors (Ogbourne & Antalis, 1998). Recently, newly discovered silencer regions are thought to be bifunctional regulatory elements, that can also act as enhancers (Gisselbrecht et al., 2020). A schematic of common regulatory elements in eukaryotic transcription are depicted in **Figure 1**.

The Pol II holoenzyme is responsible for the transcription of all protein-coding genes in eukaryotes. Prior to initiation of transcription, Pol II and general transcription factors (TFIID, TFIIA, TFIIB, TFIIF, TFIIE, TFIIH/TFIIK) assemble on promoter regions to form a pre-initiation complex. Transcriptional activation starts with the binding of activator transcription factors to enhancer and proximal regions within the promoter of a specified gene; these transcription factors can begin the process of the recruitment of co-activators that modify chromatin structure and increase accessibility of the gene region that will be transcribed by the Pol II (Vernimmen, Gobbi, Sloane-Stanley, Wood, & Higgs, 2007; Vierstra, Wang, John, Sandstrom, & Stamatoyannopoulos, 2014). A simplified model of transcription initiation is depicted in **Figure 2**.

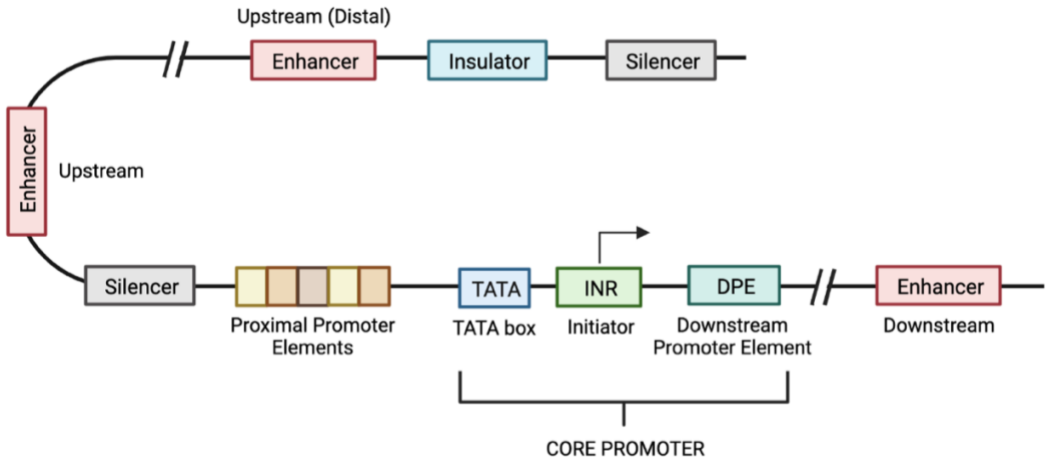

Figure 1: Schematic representation of the cis-regulatory elements involved in transcription.

The core promoter region comprises of binding sites for general transcription factors, while proximal promoter elements bind specific transcription factors. Transcriptional activation starts with the binding of activator transcription factors to enhancer and proximal regions within the promoter of a specified gene; these transcription factors can begin the process of the recruitment of co-activators that modify chromatin structure and increase accessibility of the gene region that will be transcribed by the Pol II. The transcription start site is indicated by an arrow. Figure recreated in BioRender after adaptation from **Levine & Tjian, 2003**.

1.2.2 Cis-Regulatory Elements and Sequence-Specific Transcription Factors

As previously mentioned, the regulation of transcription also involves a combination of specific transcription factors known as activators and repressors, that bind to their target sequences in regulatory regions and modulate the activity of the basal transcriptional machinery (Soutourina, 2018; Vernimmen & Bickmore, 2015). Cis-acting regulatory elements are short sequence motifs that bind general and specific transcription factors during transcription initiation. Some transcription factors function both as activators and repressors, alluding to their bifunctionality, reflecting the differential expression of activator and repressor transcription factors in different tissues (Mika & Lynch, 2016). Interestingly, differentially expressed transcriptional cofactors have also been reported to convert activators to repressors (Jiang, Cai, Zhou, & Levine, 1993). A recent report even suggests that one element can function as an enhancer of one gene and a silencer of another in the same cell type, possibly due to interference of intragenic enhancer transcription (Cinghu et al., 2017).

Generally, specific transcription factors contain a DNA-binding domain (DBD), an effector domain (such as an activation or a repression domain), a nuclear localization sequence (NLS), and a regulatory domain (Zabidi & Stark, 2016). Although, the presence of a DBD facilitates DNA binding, certain transcription factors that do not have a DBD can associate with DNA through a DNA binding partner. Additionally, transcription factors can be classified based on their binding sequence motifs and characterization of their DBD. The binding affinity to a sequence motif and DNA flexibility heavily guide the interactions between transcription factors and DNA (Dror, Golan, Levy, Rohs, & Mandel-Gutfreund, 2015). A single transcription factor can recognize multiple DNA binding motifs, with varying affinity for binding to each motif. Similarly, the

binding of one transcription factor can influence DNA flexibility in a manner that promotes the binding of a second transcription factor and related co-activators or co-repressors (Inukai, Kock, & Bulyk, 2017; Morgunova & Taipale, 2017). The functions of specific transcription factors can be further modulated by transcriptional co-regulators, which can interact with transcription factors and participate in transcriptional regulation (Levine & Tjian, 2003).

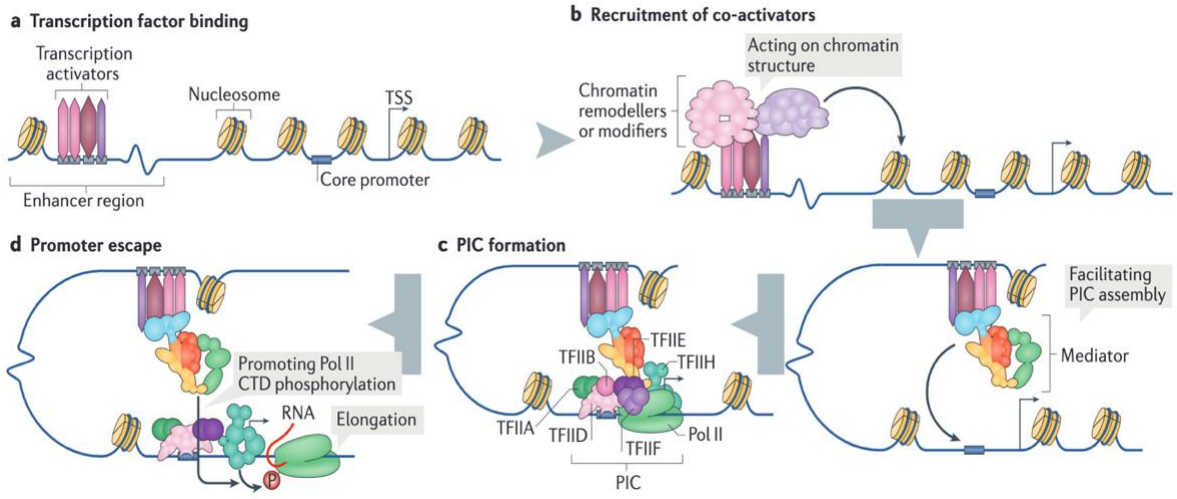

Figure 2: Simplified model of transcription initiation by RNA polymerase II in eukaryotes.

(a) Transcription factors bind to upstream or downstream enhancer regions. **(b)** Specific transcriptional factors recruit co-activator complexes to alter chromatin structure which increases accessibility. **(c)** Assembly of the pre-initiation complex (PIC) with RNA polymerase II (Pol II) and general transcription factors (in order of binding: TFIID, TFIIA, TFIIB, TFIIF, TFIIE, and TFIIH/TFIIK, which contains cyclin-dependent kinase (CDK)). **(d)** In the presence of ATP, DNA is opened by TFIIH to form a 'transcription bubble' and CDK phosphorylates Pol II to begin transcription elongation. Figure is from **Soutourina, 2018**.

1.3 Mammalian Cardiac Development

The mammalian heart develops from specified mesodermal cells from the primitive streak, which is positioned at the posterior of the epiblast. Normal cardiac development is the outcome of a sequence of coordinated cell fate decisions and morphogenetic events. Gastrulation in rodents

like mice typically occurs over three days from embryonic day (E) 6.25 to E9.5 (Tam & Behringer, 1997). The mesodermal cells migrate to form the anterolateral plate mesoderm and are patterned into progenitor cells for the organs. Following this, the mesoderm migrates towards the midline at E7.5 and fusion at the midline of the embryo leads the development of the linear heart tube, which is further elongated by the addition of the secondary heart field (Abu-Issa & Kirby, 2007). After fusion of the secondary heart field, the linear heart tube becomes functional and begins pumping blood from the venous region towards the arterial region at E8.5. This results in the development of the first formal cardiac structures. After this, the heart tube undergoes morphogenesis and begins to expand outward as the chambers of the heart begin to mature by E9.5, with ventricles forming by E10.5 (Paige, Plonowska, Xu, & Wu, 2015). Development of the mammalian heart is a complex process that requires precise coordination of cardiomyocyte specification, proliferation, differentiation, survival, and growth. As such, the cardiac gene regulatory network must interconnect with signaling pathways and their downstream effectors to ensure proper regulation of gene expression.

1.4 Overview of the MEF2 Transcription Factor

The MEF2 family of transcription factors have important roles in cellular development and post-natal adaptation with effects on cell differentiation, proliferation, migration, metabolism and apoptosis (Pon & Marra, 2016). MEF2 was initially discovered due to its DNA binding activity on an A/T-rich sequence upstream of the transcriptional start site of the *ckm* promoter. MEF2 transcription factors were first characterized by their ability to promote myogenic differentiation *in-vitro* when serum withdrawal prompted conversion of cultured fibroblasts into developing myocytes leading to the expression of myocyte related genes like myosin heavy chain (Edmondson

& Olson, 1989; Gossett, Kelvin, Sternberg, & Olson, 1989). Initial investigations suggested an overlap of MEF2 with Serum Response Factor (SRF) due to the shared presence of a MADS (MCM1, Agamous, Deficiens, SRF) box, a conserved DNA binding domain that is shared by proteins in the MADS box family. However, further analysis indicated that the MEF2 activity was specific to the consensus sequence of $CTA(A/T)_4TAG$, which is a different consensus sequence from SRF.

MEF2 is essential for the development of the heart and has a fundamental role in myocyte differentiation. As such, MEF2 was discovered as able to induce cell differentiation into the myogenic lineage as the expression of a MEF2 dominant negative protein blocked myocyte differentiation (Ornatsky & Mcdermott, 1996). It is also important for modulating the transcriptional response to varying physiological and pathological adaptations of the heart (Desjardins & Naya, 2016; Hashemi, Salma, Wales, & Mcdermott, 2015; Hashemi, Wales, Miyake, & Mcdermott, 2015).

Since the initial identification of the ability of MEF2 factors to engage in DNA binding to function as a transcriptional switch, over 80 genes have been established as direct transcriptional targets of MEF2 through transcriptome and promoter analyses (Black & Cripps, 2010). Cardiac muscle transcriptome studies have implicated *kf2*, *junb*, *alas2* and *rarres2* as direct transcriptional targets of MEF2 through a global MEF2 target gene transcriptome analysis (Wales et al., 2014). However, many transcriptional gene targets of MEF2 remain to be further characterized.

1.4.1 Structure of MEF2

MEF2 is a member of the MADS (MCM1, Agamous, Deficiens, SRF) box family of transcription factors that contain a conserved protein domain and recognize an A/T rich DNA binding motif. The MEF2 protein domains can be divided into three regions: The MADS box and MEF2 domain in the N-terminus, both regulate DNA binding, dimerization and cofactor interaction, and a transcriptional activation domain (TAD) in its C-terminus, that can regulated by a variety of post-translational mechanisms (Black & Olson, 1998; Desjardins & Naya, 2016).

The MADS and MEF2 domains are highly conserved across all species for all MEF2 isoforms (MEF2A, MEF2B, MEF2C, and MEF2D), while the C-terminus is not, as it contains the nuclear localization sequence. The MADS and MEF-2 domains are critical for the recognition of the binding motifs on DNA with abundant A/T DNA sequences to the consensus sequence to regulate the dimerization of MADS box proteins and allow interaction of MEF2 with other co-factors (Yu et al., 1992). A schematic diagram of all four MEF2 isoforms is depicted in **Figure 3**.

The MADS domain bind DNA as dimers as part of a DNA-binding complex with other DNA-binding proteins. The MADS domain is a 56-residue motif consisting of a pair of antiparallel coiled-coil α-helices against an antiparallel two-stranded β-sheet. This β-sheet of the motif is also involved in inter-protein interactions with other accessory proteins. The MADS dimerization occurs along the side of the monomer involving the α-helices and β-sheet, causing the DNA to bend around the MADS box. The N-terminus strand of the MADS region often passes over and interacts with the DNA backbone (Luscombe, Austin, Berman, & Thornton, 2000). In addition to this, the conserved sequence within MEF2 domain allows for the formation of homodimers or heterodimers structures within the specific isoforms of MEF2 or heterodimers with other

molecules (Ornatsky & Mcdermott, 1996). Additionally, the heterogeneity of the C-terminus sequence provides the opportunity for MEF2 isoforms to differentially regulate the same genes through patterns of alternative splicing and extensive posttranslational modifications like phosphorylation (Molkentin & Olson, 1996).

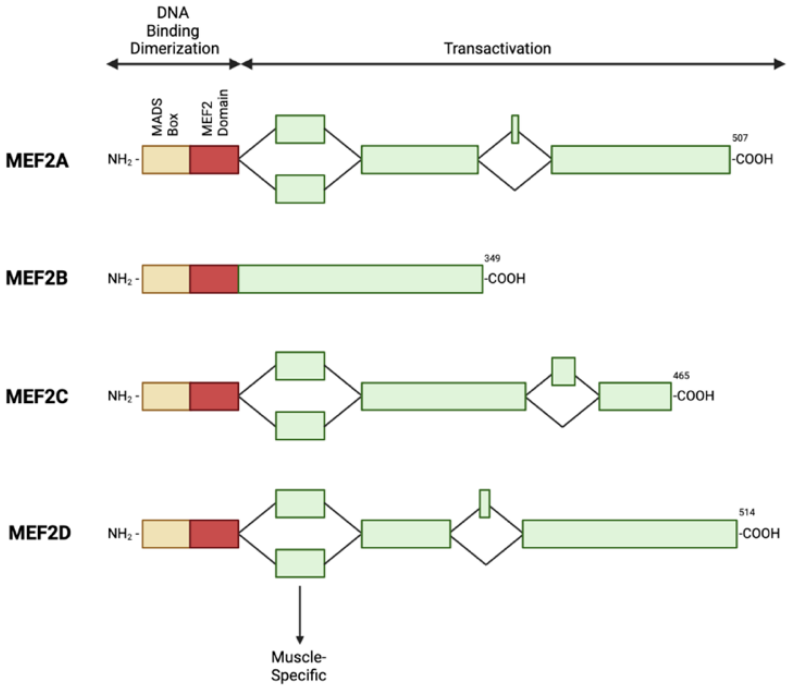

Figure 3: Schematic diagrams of the four MEF2 factors.

Structures of the four vertebrate MEF2 gene products are shown. Following the N-terminus, the DNA binding and dimerization region consists of the MADS box and MEF2 Domain. The transactivation domain featuring alternative exons within the C-terminus are indicated, along with the number of amino acids in the protein. Figure recreated in BioRender after adaptation from **Molkentin & Olson, 1996**.

1.4.2 MEF2 in Vertebrate Cardiac Development

Most vertebrate genomes contain at least four *Mef2*-encoding genes (MEF2A, MEF2B, MEF2C, and MEF2D), and the expression of *Mef2* genes are regulated at the transcriptional and translational level. Prior to expression of sarcomeric genes like cardiac α-actin, MEF2B and

MEF2C are the first isoforms expressed in the cardiac mesoderm at E7.5 in the developing mouse embryo (Edmondson, Lyons, Martin, & Olson, 1994). Most notably, after E8.5 all four isoforms of the *Mef2* genes are expressed throughout the developing heart (**Figure 4**). Postnatally, MEF2A and MEF2D are the most abundant isoforms in the heart (Naya, Wu, Richardson, Overbeek, & Olson, 1999). Interestingly, MEF2C expression has also been detected in postnatal cardiomyocytes, and is believed to play a role in homeostasis (Pereira et al., 2009).

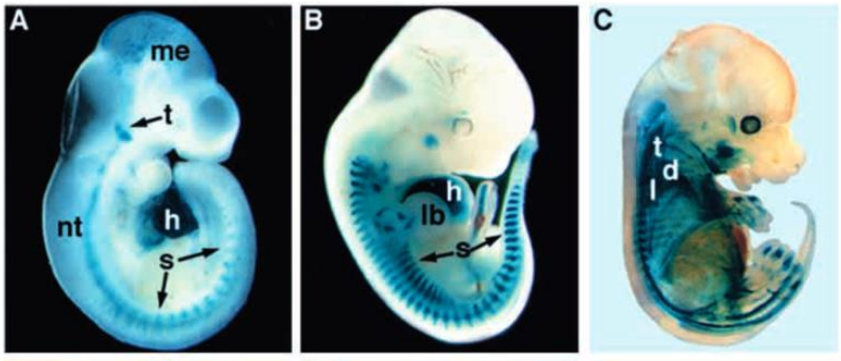

Figure 4: Expression of 3x-Des-MEF2-lacZ reporter construct in transgenic mice embryos.

Mouse embryos (E9.5, E11.5 and E14.5 from **left to right**) showing early robust staining of MEF2 transcriptional activity in the heart (h), somites (s), neural tube (nt), mesencephalon (me), trigeminal ganglia (t), limb buds (lb), trapezius muscle (t), lattisimus dorsi muscle (l) and deltoid muscle (d). Figure is from **Naya et al., 1999**.

To investigate the *in-vivo* role of the MEF2 transcription factor family, knockout mice have been established. All MEF2 family members are expressed during cardiac development, however, MEF2A and MEF2D are the primary MEF2 factors expressed in the adult vertebrate heart. Animal studies have shown that mice deficient in MEF2A exhibit sudden perinatal lethality and have significant post-natal dilation of the right ventricle (Naya et al., 2002). While a small percentage of MEF2A knockout mice are viable into adulthood, the heart often has mitochondrial deficiency

and conduction defects. Interestingly, upon MEF2A knockdown, the expression of MEF2D was upregulated, showing a possible compensation with a different isoform of MEF2. Unfortunately, MEF2B knockout mice have revealed very little about the role of MEF2B in development and the characterization of the model remains to be investigated (B. L. Black & Olson, 1998). However, it is reported that MEF2B knockout mice are viable and lack any specific muscle phenotype. Additionally, it was reported that absence of MEF2B could be compensated by either MEF2A or MEF2C in cardiac development (Lin, 1997).

Animal studies have shown that a MEF2C knockout results in embryonic lethality due to myocardial impairments. The embryos are prone to cardiac looping defects, and disruption in right ventricle formation *in-utero*. However, cardiomyocyte-specific deletion of MEF2C at E10.5 using transgenic mice results in viability and normal cardiac development (Vong, Ragusa, & Schwarz, 2005). This suggest that MEF2C is dispensable after early embryonic development or that it is compensated by the other MEF2 isoforms. More notably, animal studies have shown that mice deficient in MEF2D exhibit normal cardiac structure and function. However, when the MEF2D knockout mice were subjected to specific cardiac stress, they displayed attenuated hypertrophy and fibrosis showing resistant to cardiac hypertrophy and pathological remodeling of the heart (Kim et al., 2008). Additionally, an acute depletion of MEF2D in neonatal cardiomyocytes *in vitro* results in cell death (Estrella, Clark, Desjardins, Nocco, & Naya, 2015).

In addition to the loss of function studies, the MEF2 proteins have also been overexpressed in neonatal cardiomyocytes and the heart. The *in-vitro* overexpression of MEF2A, MEF2C, and MEF2D have resulted in similar phenotypes, which have included cardiomyocyte elongation and sarcomere disorganization leading to cardiomyocyte dilation (Kim et al., 2008; Van Oort et al.,

2006; Xu et al., 2006). MEF2A and MEF2C overexpression resulted in dilated cardiomyopathy and MEF2D overexpression resulted in atrial enlargement and extensive fibrosis. However, it is important to clarify that MEF2 was expressed at supra-physiological levels potentially overcoming isoform-specific gene regulatory effects.

1.5 Regulation of MEF2 Transcriptional Activity

MEF2 functions as a transcriptional switch that can potently activate or repress transcription through interactions with co-factors that can be positive and negative regulators of transcription (Kohli et al., 2012; Wales et al., 2014). The regulation of the transcriptional activity of the MEF2 transcription factors is complex. As previously mentioned, the TAD in the C terminus of MEF2 can regulated by different extracellular stimuli and pathways, alternatively spliced variants of MEF2 isoforms, dimerization, and various form of post-transcriptional and post-translational modifications mechanisms (Molkentin & Olson, 1996).

The MADS and MEF2 domains at the N terminus have additional functions beyond DNA binding and dimerization. The majority of characterized interactions between MEF2 and other transcription factors that serve as co-factors are mediated by regions within the MADS domain (McKinsey, Zhang, Lu, & Olson, 2000). There are also critical sites of phosphorylation and dephosphorylation on serine and threonine residues. Most importantly, phosphorylating kinases and dephosphorylating phosphatases for MEF2 are important for the regulation of a variety of processes like modulation of DNA-binding affinity, association of MEF2 with transcriptional co-activators and co-repressors, acetylation and sumoylation, nuclear and cytoplasmic trafficking and caspase-mediated degradation (J. Han, Jiang, Li, Kravchenko, & Ulevitch, 1997; Ornatsky & Mcdermott, 1996; Perry et al., 2009; Shalizi et al., 2006; Tang et al., 2005; Yu, 1996).

1.5.1 p38 MAPK Signal Transduction Pathway

The p38 mitogen-activated protein kinase (p38 MAPK) pathway participates in a signalling cascade that is known for controlling responses to cytokines and cellular stresses. p38 MAPK is activated by cellular stresses including osmotic shock, oxidative stress, inflammatory cytokines, lipopolysaccharides (LPS), UV light, growth factor and GPCR stimulation. There are four p38 MAP kinases in mammalian cells, p38α (MAPK14), p38β (MAPK11), p38γ (MAPK12 or ERK6), and p38δ (MAPK13) (Young, 2013). The p38 MAPKs regulate downstream targets including several kinases, transcription factors phosphorylated by p38 MAPK and cytosolic proteins. Several direct substrates of p38α have been identified, one such target is MEF2 (**Figure 5**). There are eight reported sites for phosphorylation in the TAD of MEF2 (M. Zhao et al., 1999).

The activation of p38 leads to phosphorylation of a conserved sequence in the C-terminal transcriptional activation domain of MEF2 (McKinsey, Zhang, & Olson, 2002). There is a p38α and p38β specific activation of MEF2A and MEF2C. Activated p38 MAPK phosphorylates Threonine 312, 319 and Serine 453 in the MEF2A TAD and phosphorylates Threonine 293, 300 and Serine 387 in the MEF2C TAD (M. Zhao et al., 1999). Phosphorylation by p38 MAPK in MEF2A and MEF2C enhance the transcriptional activity of MEF2 (McKinsey et al., 2002). Similarly, ERK5 is a MEF2 co-activator, and its activation leads to the formation of a complex with MEF2, resulting in transcriptional activation (Lu, McKinsey, Nicol, & Olson, 2000)

Interestingly, p38 MAPK inhibitors have proven to reasonably selective for teasing apart the p38 MAPK signaling pathway. One such compound is SB203580, which is thought to preferentially bind to the inactive form of p38 MAPK, particularly p38α and p38β, but not the γ or δ homologues. SB203580 inhibits the catalytic activity of p38 MAPK by binding to the ATP-

binding pocket, however, it does not inhibit phosphorylation of p38 MAPK by upstream kinases (Cuenda et al., 1995; Goedert, Cuenda, Craxton, Jakes, & Cohen, 1997; Kumar et al., 1997; Lee et al., 1994).

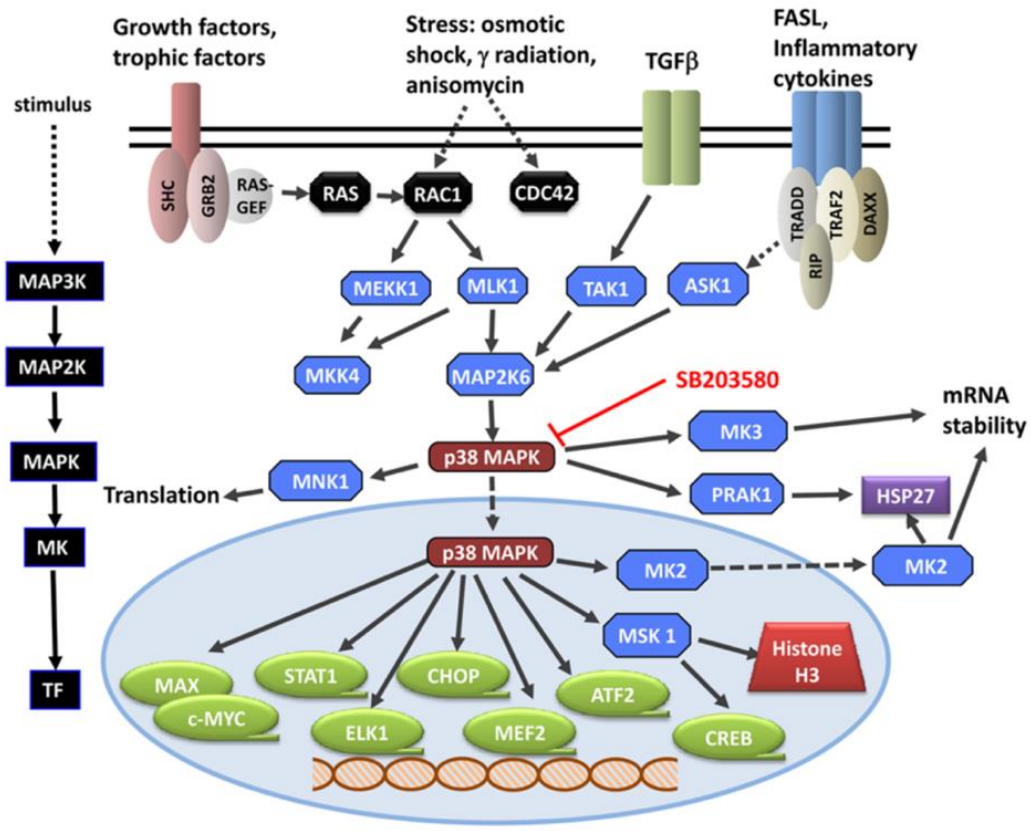

Figure 5: Overview of the p38 MAPK signal transduction pathway.

The activation of the p38 MAPK signal transduction pathway is often through extracellular stimuli, and it mediates signal transduction into the nucleus to regulate the responsive genes. Inhibition with SB203580 is highlighted in red and the direct substrates of p38α, like MEF2, are in green. Figure is from **Young, 2013**.

1.5.2 MEF2 and Chromatin Remodeling

Additionally, the MADS domain is also critical for the interaction of MEF2 with Histone acetyltransferases (HATs) and Histone deacetylases (HDACs) (Lu et al., 2000). As such, MEF2

appears to regulate the relative accessibility of promoters and enhancers to transcription machinery through chromatin acetylation and deacetylation (Jenuwein, 2001). Interestingly, this has led to the development of a dual model of function for MEF2, in which MEF2 interacts with both HATs in the context of activating gene transcription and repressing HDACs to repress gene transcription. In this model, MEF2 can bind the DNA and associate with Class II HDACs, which can repress gene expression through the recruitment of Class I HDACs. Class II HDACs repress MEF2 family members through interaction with a short amino acid sequence conserved among MEF2 factors (Han, He, Wu, Liu, & Chen, 2005). Similarly, a dissociation of the HDAC complex, allows MEF2 to bind p300/CBP and activate gene expression (Haberland et al., 2007). The activation of the CaMK signaling pathway attenuates the association of HDACs with MEF2, allowing for MEF2 activation (Lu et al., 2000; Mckinsey, Zhang, & Olson, 2000).

Furthermore, Class II HDACs are important regulators of transcription in the prenatal and postnatal heart (Verdin, Dequiedt, & Kasler, 2003). It is established that dissociation of class II HDACs from MEF2 downstream is a key stimulant of postnatal MEF2 transcriptional activity due to hypertrophic signaling (Lu et al., 2000; McKinsey & Olson, 2005; McKinsey et al., 2000) The hypertrophic stress stimulus activates many protein kinases that phosphorylate class II HDACs on specific amino acid residues which serve as docking sites for adaptor protein 14-3-3, resulting in nuclear export and MEF2 activation (Backs & Olson, 2006; Parra & Verdin, 2010). The dual model of duction for MEF2 is illustrated in **Figure 6**.

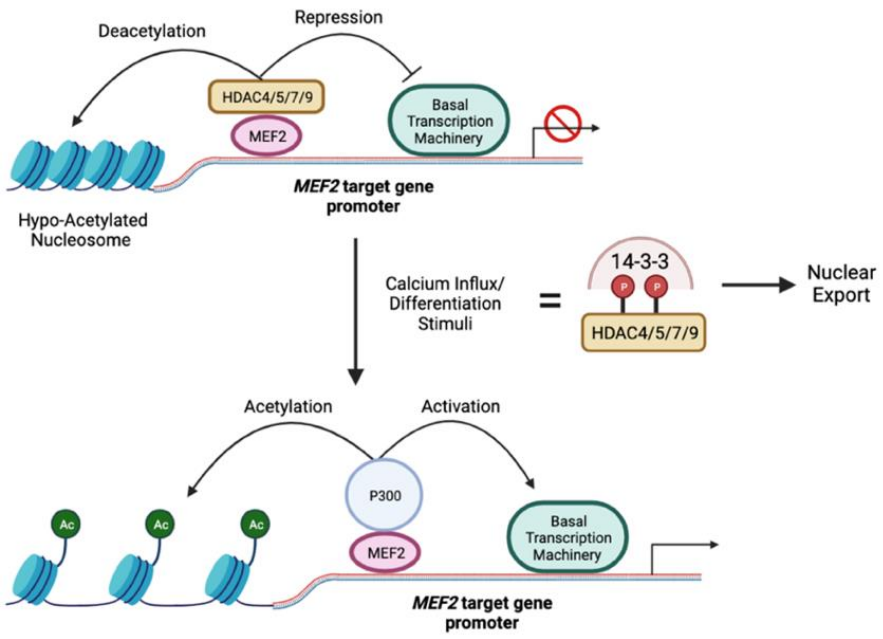

Figure 6: Dual activator and repressor functions of MEF2.

In the dual model, MEF2 can bind to DNA and associate with HDACs to repress gene expression (**top image**). Various stimuli can activate Ca2+/Calmodulin-dependent protein kinase signaling, which phosphorylates the HDACs, promoting their association with 14-3-3 proteins and resulting in export from the nucleus. As such, without the presence of HDACS, MEF2 can bind to DNA and associate with HATs like p300 and become an activator of gene transcription (**bottom image**). Figure recreated using BioRender from **McKinsey et al., 2002**.

1.6 MEF2 Global Gene Regulatory Network

Through comprehensive genome-wide studies in *D. melanogaster*, the C2C12 skeletal myoblast cell line, and in HL-1 cardiac atrial cell line, researcher have uncovered that the global mechanisms of gene regulation involving MEF2 extend beyond its role as an essential transcriptional factor (Blais et al., 2005; Estrella et al., 2015; Paris, Virtanen, Lu, & Takahashi, 2004; Sandmann et al., 2006). Current understandings of the regulatory actions of MEF2 have moved away from the approach that MEF2 is an exclusive transcriptional regulator of structural and myogenic genes. Of most importance, research has indicated that MEF2 also has a strong role

in global gene regulation, including genome-wide binding and regulating target gene expression for an array of cellular processes including signalling transduction cascades, transcription factors, muscle differentiation, and the neuromuscular junction (**Figure 7**).

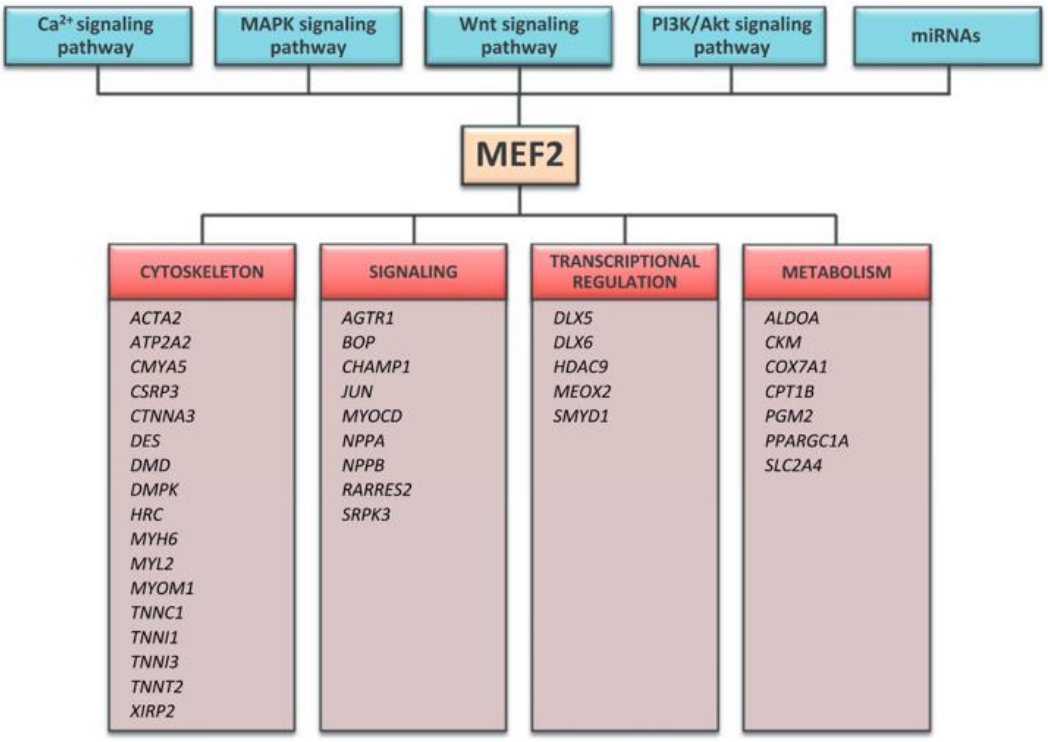

Figure 7: Overview of the signalling pathways that can activate MEF2 and direct target genes of MEF2 identified in the heart.

The MEF2 family is closely associated with various signaling pathways, including Ca2+ signaling, MAP kinase signaling, Wnt signaling, PI3K/Akt signaling, in addition to microRNAs. Figure is from **Filomena & Bang, 2018.**

1.6.1 Cardiac MEF2 Protein:Protein Interactions

There is extensive experimental data to support the role of MEF2 in cardiac gene regulatory networks. ChIP-on-chip and RNAi methodologies were utilized to characterize the genome-wide binding of MEF2 in the cardiac regulatory network to identify unique target genes regulated by

the core mammalian cardiac DNA-binding transcription factor network of GATA4, MEF2, CSX/NKX2.5, and SRF. The results of this global gene analysis indicated that different cohorts of target gene are regulated by distinct networks of the cardiac transcription factors. In particular, it was found that MEF2A and NKX2.5 co-regulated genes belonging to muscle differentiation and heart looping pathways (Schlesinger et al., 2011). Similarly, a streptavidin pulldown of overexpressed BirA biotinylation peptide-tagged transcription factors and ChIP-seq in HL-1 cells have indicated that there are strong interactions between MEF2A and various transcription factors like GATA4, CSX/NKX2.5, and SRF (A. He, Kong, Ma, & Pu, 2011).

Additionally, ChIP-exo experiments were also used to identify and compare the genome-wide, direct target genes of MEF2A in neonatal cardiomyocytes and C2C12 cells. The results indicated that the MEF2A bound regions in cardiomyocytes had an overrepresentation of transcription factor AP-1, CREB, BACH, and ERE binding sites. Furthermore, a corresponding gene ontology analysis revealed that the most significantly enriched genes bound by MEF2A in neonatal cardiomyocytes are involved in actin and cytoskeleton organization (Estrella & Naya, 2014; Ewen, Snyder, Wilson, Desjardins, & Naya, 2011; Wales et al., 2014). Most interestingly, a mathematical modeling with Gibbs sampling and linear regression was also utilized to identify putative significantly enriched cardiac transcription factor binding sites in the human genome active in cardiac development and differentiation. The results indicated that MEF2 and SRF binding sites obtained the maximum positive weight scores.

This shows that MEF2 is a major player in cardiac gene regulatory networks, in addition to MEF2A binding strongly overlapping with other transcriptional network components and interacts with multiple transcription factors to regulate downstream gene expression.

1.7 Thesis Rationale

1.7.1 The MEF2A Interactome and Functional Protein Interactions with STAT3

The MEF2 transcription factor is at the center of an evolutionary conserved regulatory network defining cardiac-specific gene expression encoding structural and regulatory proteins (Olson, 2006). The McDermott lab has implicated the MEF2A transcription factor with the regulation of genes expressed commonly during cardiac hypertrophy, and a previously conducted MEF2 transcriptome analysis highlighted that 168 gene targets within the neonatal cardiomyocytes were significantly impacted by the MEF2A depletion (Tobin et al., 2017) (**Figure 8A**). Due to the fundamental role of MEF2A in cardiomyocyte development, disease and homeostasis, the lab has been interested in further characterizing the MEF2A cardiac protein interaction network.

The experimental work of doctoral student Amira Moustafa in the McDermott lab sought to generate a systematic unbiased screen of the MEF2 interactome in cardiomyocytes using affinity purification coupled with quantitative proteomics. The goal of this strategy was to identify key MEF2A protein interactions in primary cardiomyocytes, and reveal potential regulatory roles in cell death, inflammatory and stress response, and actin dynamics. This experiment identified 56 proteins that had enriched with MEF2A and many of these interactions are novel. Following bioinformatic analysis, attention was directed to a novel interaction between MEF2A and STAT3, due to both factors being previously identified independently as key regulators of cardiomyocyte gene expression (Moustafa et al., *in press*). It was shown that a potential interaction between MEF2 and STAT3 proteins exerts a level of executive control over several important biological processes in neonatal rat ventricular cardiomyocytes that are key to cell survival and adaptive immune response mechanisms related to cardiac dysfunction and pathology (Moustafa et al., *in press*).

Following the interactome studies, a MEF2 luciferase reporter gene assay was conducted to assess the functional effect of STAT3 on MEF2-dependent promoter activity. Additionally, through the gain of function (ectopic overexpression), loss of function (siRNA depletion) and pharmacologic inhibition (STAT3 inhibitor XIII, C188-9) experiments on MEF2-luciferase dependent promoter regions, Amira Moustafa confirmed that STAT3 also represses MEF2 transactivation function in NRVMs. Currently, it remains to be elucidated if this interaction is physical or bridged by other factors. The repressive effect of STAT3 on MEF2 transactivation are more robust than the reciprocal effect of MEF2A on STAT3 activity. Despite this, STAT3 was chosen to be evaluated as target within the MEF2A regulatory mechanism mediating transcriptional regulation.

1.7.2 The MEF2A and STAT3 Transcriptome

Building on this, recent work in the McDermott lab was focused on further investigating the potent role played by both MEF2A and STAT3 in cardiomyocyte biology due to the repressive effect of STAT3 on MEF2. As such, primary cardiomyocytes were depleted of STAT3 using siRNA technology. The STAT3 transcriptome analysis highlighted that 111 gene targets within the neonatal cardiomyocytes were significantly impacted by the STAT3 depletion (Moustafa et al., *in press*) (**Figure 8B**). Following this, the transcriptome data from both the MEF2A and STAT3 depleted cardiomyocytes were integrated to identify key gene target that appeared to be co-regulated by both MEF2A and STAT3. The integrated comparative analysis of the transcriptomes of MEF2A and STAT3 siRNA depleted cardiomyocytes provided the ability to further assess potential overlap of gene regulatory programs or mechanisms shared between MEF2A and STAT3.

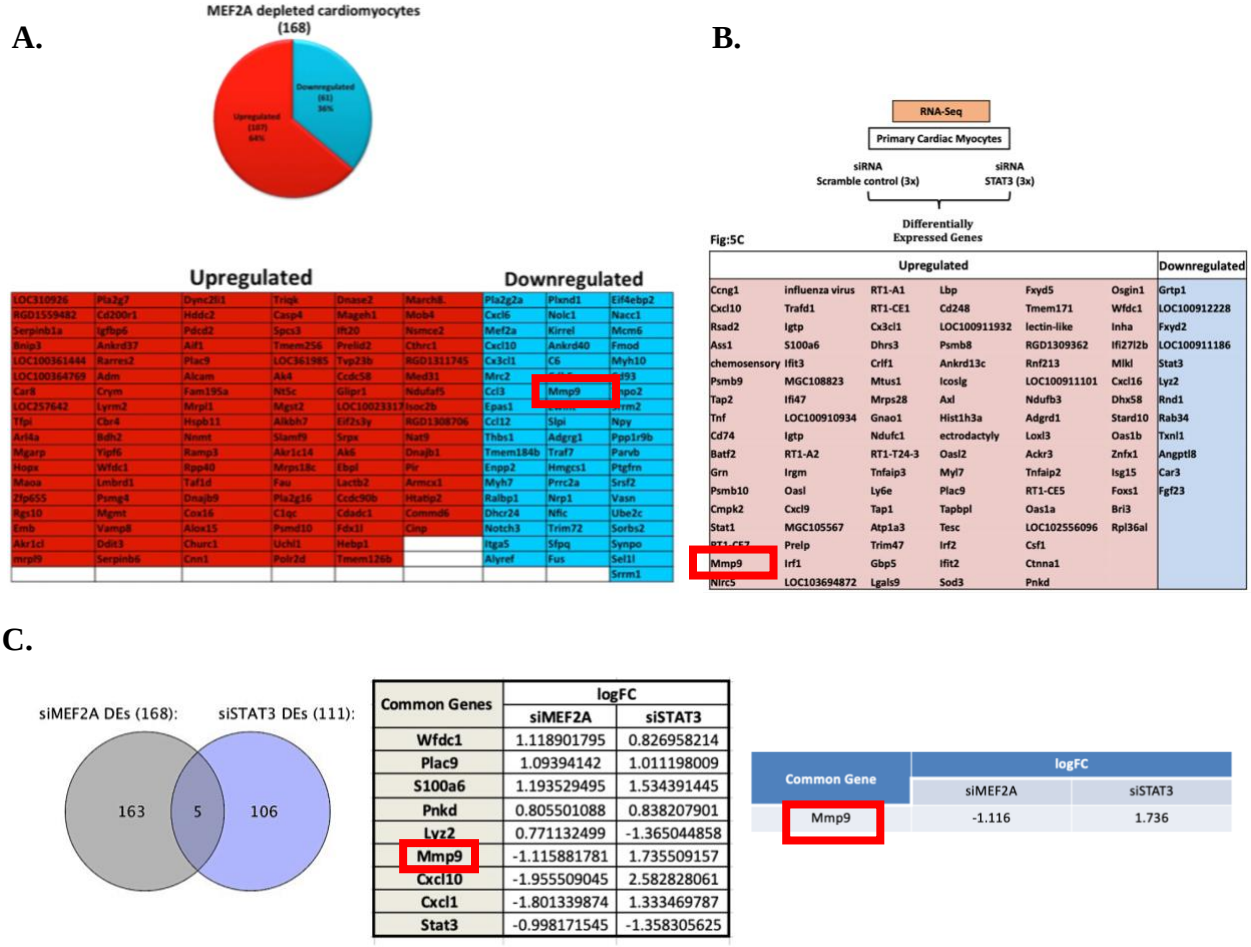

Common Genes	logFC	
	siMEF2A	siSTAT3
Wfdc1	1.118901795	0.826958214
Plac9	1.09394142	1.011198009
S100a6	1.193529495	1.534391445
Pnkd	0.805501088	0.838207901
Lyz2	0.771132499	-1.365044858
Mmp9	-1.115881781	1.735509157
Cxcl10	-1.955509045	2.582828061
Cxcl1	-1.801339874	1.333469787
Stat3	-0.998171545	-1.358305625

Common Gene	logFC	
	siMEF2A	siSTAT3
Mmp9	-1.116	1.736

Figure 8: MEF2A and STAT3 siRNA mediated depletion transcriptome integration.

(A) Summary list of upregulated (red) and downregulated (blue) genes in response to si-RNA mediated MEF2A depletion in primary cardiomyocytes identified by RNA-seq analysis. Figure is from **Tobin et al., 2017**. **(B)** Summary list of upregulated (red) and downregulated (blue) genes in response to si-RNA mediated STAT3 depletion in primary cardiomyocytes identified by RNA-seq analysis. Figure is from **Moustafa et al., *in press***. **(C)** Left: Venn diagram representing the common genes between the two data sets: siMEF2A DEs, and siSTAT3 DEs. Center and Right: Tables represents logarithmic fold changes in common gene and MMP9 RNA in MEF2A and STAT3 depleted conditions in NRVM. Data in **8C** was generated and figures were created by **Amira Moustafa**. (**DE**: Differential expression, **FC**: Fold Change).

The analysis revealed four genes of particular interest that were both upregulated by STAT3 depletion and downregulated by MEF2A depletion. The genes exhibiting this pattern of expression were C-X3-C Motif Chemokine Ligand 1 (CX3CL1), C-X-C Motif Chemokine Ligand 10 (CXCL10), lysozyme 2 (LYZ2), and Matrix Metalloproteinase 9 (MMP9), all of which have implications for heart disease and cardiac failure (Moustafa et al., *in press*) (**Figure 8C**). CX3CL1, CXCL10 and MMP9 are primarily related to the innate immune response consistent with a previously documented cardioprotective role of STAT3 (Prabhu & Frangogiannis, 2016).

MMP9 has shown to promote cardiac remodeling through the regulation of extracellular matrix degradation and through the activation of a variety of chemokines and cytokines. Previous studies have revealed that MMP9 is a potential biomarker for cardiac remodeling linked with inflammation, diabetic complications, extracellular matrix degradation and synthesis, and cardiac dysfunction (Yabluchanskiy, Ma, Iyer, Hall, & Lindsey, 2013). Thus, the experimental goals for this project may identify clinically relevant data.

Matrix metalloproteinases (MMPs) like MMP9 are zinc-dependent endopeptidases that cleave structural elements of the extracellular matrix (ECM) and process a variety of non-ECM substrates including cytokines, chemokines, growth factors, and adhesion molecules that alter cellular migration, adhesion, differentiation, growth, inflammatory processes, activation and apoptosis (Hideaki Nagase & Woessner, 1999; Visse & Nagase, 2003). The proteolytic activities of MMPs influence essential cellular processes; in addition to many fundamental physiological events involving tissue remodeling for development, involution, morphogenesis, and repair (H Nagase, Visse, & Murphy, 2006). MMP9 is secreted by cardiomyocytes with increases in the MMP9 protein level correlating with ventricular enlargement and dysfunction following a

myocardial infarction (Squire, Evans, Ng, Loftus, & Thompson, 2004). As such, we found MMP9 to be of particular interest in further investigating its regulation by MEF2A and STAT3.

1.8 Research Aims and Hypothesis

Based on the evidence from the preliminary data, **it is hypothesized a protein:protein interaction between MEF2A and STAT3 transcription factors regulates MMP9 gene expression in cardiomyocytes**. In combination with the preliminary transcriptome and interactome data, the purpose of this thesis is to interrogate the MEF2 and STAT3 protein-protein interaction in the context of global cardiomyocyte gene regulation by further investigating their regulation of MMP9, which is one of the three genes exhibiting upregulation by STAT3 depletion and downregulation by MEF2A depletion. This thesis investigates the effect of the hypothesized STAT3:MEF2A complex on both the mRNA and protein level of MMP9. Based on the hypothesis, the three objectives of this thesis are as follows:

1. Study the role of MEF2A and STAT3 on MMP9 promoter activity using a luciferase reporter gene assay-based system in primary neonatal rat ventricular cardiomyocytes (NRVMs).

2. Conduct siRNA mediated gene silencing of MEF2A and STAT3 and treat NRVMs with p38 MAPK (SB203580) and STAT3 (C188-9) inhibitors to study their impact on MMP9 promoter activity in NRVMs. Evaluate changes in relative MMP9 protein content in response to the depletions and pharmacological treatments.

3. Use RT-qPCR to evaluate changes in relative MMP9 mRNA levels in NRVMs under conditions of siRNA mediated gene silencing of MEF2A and STAT3.

2. MATERIALS AND METHODS

2.1 Experimental Animals

Male and female Sprague Dawley rats (*Rattus norvegicus domestica*) were housed in temperature and humidity-control rooms (21 ± 2°C, 35-40%) with a daily 12:12 hour light-dark cycle with access to regular chow diet ad libitum in the animal care facility of York University in accordance with the guidelines of the Canadian Council on Animal Care. All breeding and experimental protocols were approved by the Animal Care Committee of York University. Every 3 weeks, a female rat was co-housed with a male rat for a 24-hour period during which mating, and presumably, conception occurred. Cage cards were updated with dates of pairing, litter delivery, and removal of the rat pup litter after birth.

2.2 Streaking and Isolating Bacteria on an Ampicillin Selective Agar Plate

To obtain well-isolated discrete colonies from a stab culture of bacteria containing the plasmid of interest pGL2Basic-MMP9-Luciferase (Addgene, #53434), the quadrant streak technique was used. Ampicillin selective agar plates were prepared by autoclaving 6 g LB agar in 400 mL of ddH_2O. Once the mixture was cooled to 60°C, 400 µl of ampicillin (100mg/mL) was added and the mixture was poured into 100 mm petri dishes and left to solidify. Using a sterile pipette tip, the bacteria growing within the punctured area of the stab culture was touched and gently streaked over the first quadrant. Following this, a new sterile pipette tip was dragged through the streak on the first quadrant and streaked over the second quadrant. This sequential dilution was repeated over the third and fourth quadrants. The plates were incubated upside-down overnight at 37ºC. In the morning, single colonies were visible for plasmid DNA isolation.

2.3 Large Scale Plasmid Isolation (Maxiprep)

Single *E. coli* colonies growing on the ampicillin selective LB agar plate were picked and cells carrying the plasmid of interest were grown in 250 mL of LB Broth with the ampicillin (100 mg/mL) as the selective antibiotic. Cultures were incubated overnight at 37ºC with shaking at 250 rpm. The following day, the cultures were transferred into multiple 50 mL conical polypropylene tubes and centrifuged at 6000 x g for 10 minutes to pellet cells. Plasmid DNA was obtained with the Qiagen Plasmid Maxi Kit following the manufacturer's protocol (Qiagen, #12162). DNA concentration, absorbance ratio, and 260nm/280nm was measured using a NanoDrop 2000 spectrophotometer. The plasmid quality was evaluated by separating 0.5 µg of the sample on an agarose gel at 100 V for 35 minutes.

2.4 *E. coli* Plasmid Transformation

E. coli cells were transformed to amplify reporter constructs of interest: pRL-Renilla (Promega, #E2271) and pGL2Basic-MMP9-Luciferase (Addgene, #53434). 1 µL of purified plasmid DNA was added to 100 µL of thawed, chemically competent XL1-Blue *E. coli* cells and the mixture was incubated on ice for 30 minutes. Cells were heat shocked at 42ºC for 30 seconds and placed again on ice for 2 minutes. Next, cells were mixed with 200 µL of autoclaved lysogeny broth (LB) media and incubated at 37ºC for 1 hour with shaking at 250 rpm. Following incubation, 100 µL of the mixture were evenly plated on 100 mm LB agar plates with ampicillin (100 mg/mL) and incubated upside-down overnight at 37ºC. The next day, the plates were removed, wrapped in parafilm, and stored at 4°C.

2.5 Isolation of Primary Cardiomyocytes from Neonatal Rats

Primary cardiomyocytes were isolated from the hearts of 1-3 days old Sprague Dawley rat pups sacrificed by cervical dislocation. The hearts were surgically removed and washed in ice-cold sterile calcium-free and magnesium-free Hank's Balanced Salt Solution, pH 7.4 (Worthington, #LK003210). The cardiac tissue was minced into pieces less than 1 mm^3 with small scissors. The cardiomyocytes were isolated using the Worthington Neonatal Cardiomyocyte Isolation System following manufacturer's protocol (Worthington, #LK003300) and re-suspended in 10 mL Dulbecco's Modified Eagle's Medium/Nutrient Mixture F-12 (DMEM/F-12) (Gibco, #11320033) supplemented with 10% fetal bovine serum (FBS) and 1% penicillin/streptomycin (Pen-Strep) at 10,000 U/mL. The cell suspension was added to a 10 mm cell culture dish and incubated for 3 hours at 37°C in a 5% CO_2 atmosphere. The cell suspension containing the unattached cardiomyocyte was transferred to a sterile 50 mL conical polypropylene tube, and the cell culture dish with differential attachment of non-myocardial cell was discarded.

2.6 Gelatin-Coated Tissue Culture Dishes

Six-well tissue culture dishes were coated with gelatin (0.02%) and incubated overnight at 37ºC. The next day, the gelatin was removed by aspiration and tissue culture dishes were stored in the 5% CO_2 incubator at 37°C for up to 1 week. Prior to plating the cardiomyocytes, the tissue culture dishes were opened and sterilized under UV light in the biosafety cabinet for 30 minutes.

2.7 Primary Cardiomyocyte Cell Counting and Culture Plating

Cardiomyocytes were counted to ensure even seeding density of the cells during plating. 20 µL of the cardiomyocyte cell suspension was added to 20 µL of 0.4% trypan blue solution and the mixture was incubated for 1 minute. 15 µL of the mixture was loaded onto the coverslip-

covered plateau of a hemacytometer. Each 4x4 grid was viewed under microscope magnification to count the number of viable cells. Using a hand tally counter, the unstained cells within a set grid were counted. The average was taken of the four values to get the cell density per millilitre of cells in suspension. The average was multiplied by 10,000 and the dilution factor. The cells were plated in six-well plates at a seeding density of $1.5x10^5$ cells/well and left undisturbed for a 24-hour period, after which the culture media (DMEM/F-12, 10% FBS, 1% Pen-Strep) was aspirated and replaced with serum-starved media (DMEM/F-12, 1% Pen-Strep).

2.8 Plasmid DNA Transfections

Primary cardiomyocyte cells were co-transfected with the firefly luciferase gene reporter constructs and a control *Renilla* plasmid in a 1:3 ratio of 1 μg *MMP9* promoter luciferase gene construct to 0.3 μg control *Renilla* gene construct. Lipofectamine 2000 transfection reagent (Invitrogen, #11668019) was used to transfect cells by preparing two Eppendorf tubes, each containing 100 μL 1X Opti-MEM reduced serum media (Gibco, #31985070). To one tube, Lipofectamine 2000 transfection reagent (1 mg/mL) was added, and to the other, the previously mentioned 1:3 ratio of plasmid DNA was added. The contents of the tubes were combined, vortexed and incubated for 20 minutes. During this time, the culture media was aspirated from the plated cells and replaced with 1 mL Opti-MEM media. Following this, the prepared DNA-Lipofectamine solution was equally added to each well. After 8-10 hours, the Opti-MEM media was aspirated and replaced with serum-starved media (DMEM/F-12, 1% Pen-Strep). Following this, the cells were left undisturbed for a 36-hour period, after which they were harvested.

2.9 Pharmacological Treatment of Primary Cardiomyocyte Cultures

Isolated primary cardiomyocyte cells were treated with p38 MAPK inhibitor, SB203580 (Sigma Aldrich, #S8307), and its inactive analogue, SB202474 (Santa Cruz Biotechnology, #CAS172747-50-1). To inhibit the STAT3 Y705 phosphorylation, a STAT3 inhibitor XIII, C188-9 (Sigma Aldrich, #573128) was used and dimethyl sulfoxide (DMSO) (Sigma Aldrich, # 276855) and DMSO served as the vehicle control for the C188-9 drug treatment. 1 mg of SB203580 was dissolved in 265 μL of filtered DMSO for a working stock concentration of 10 mM. For a single 16-hour SB203580 treatment, 2 μL of stock was added to cells in 2 mL serum-starved media for a treatment concentration of 10 μM. 1 mg of SB202474 was dissolved in 385 μL of filtered DMSO for a working stock concentration of 10 mM. For a single 16-hour SB202474 treatment, 2 μL of stock was added to cells in 2 mL serum-starved media for a treatment concentration of 10 μM. 10 mg of C188-9 was dissolved in 1 mL of filtered DMSO for a working stock concentration of 20 mM. For a single 1-hour treatment, 1 μL of stock was first dissolved in 1 μL of filtered DMSO for 2 μL to be added to cells in 2 mL serum-starved media for a treatment concentration of 10 μM. 2 μL of DMSO was added to cells in 2 mL of with serum-starved media as a vehicle control for C188-9 treatment. In dual treatment conditions, C188-9 was added after 16-hour incubation with SB203580 without changing the media, and DMSO was added after 16-hour incubation with SB202474.

2.10 Gene Silencing with siRNA

Transient transfection of the siRNA duplexes of scrambled control, MEF2A, and STAT3 was carried out using Lipofectamine RNAiMAX (Invitrogen, #13778075). Two siRNAs (Mission® siRNA ID's: SASI_Mm01_00120787, SASI_Mm01_00120788), targeting MEF2A

were purchased from Sigma-Aldrich. They were reconstituted in nuclease free water and the concentration used was 200nM. Two siRNAs (Mission® siRNA ID's: SASI_Mm01_00041178, SASI_Mm02_00041179) targeting STAT3 were purchased from Sigma-Aldrich. They were reconstituted in nuclease free water and the concentration used was 200nM. A universal scrambled siRNA (Sigma-Aldrich, #sic001) was used as the control condition at the equivalent concentration.

Two Eppendorf tubes were prepared, each containing 90 μL 1X Opti-MEM reduced serum media (Gibco, #31985070). To one tube, the RNAiMAX transfection reagent (1 mg/mL) was added and to the other, the diluted siRNA (100-200nM) was added. The contents of the tubes were combined, vortexed and incubated for 10 minutes. During this time, the culture media was aspirated from the plated cells and replaced with 1 mL Opti-MEM media. Following this, the prepared siRNA-RNAiMAX solution was divided and equally added to each well. After 8-10 hours, the Opti-MEM media was aspirated and replaced with serum-starved media (DMEM/F-12, 1% Pen-Strep). Following this, the cells were left undisturbed for a 24-hour period, after which they were harvested. To confirm gene silencing effects, protein lysates were prepared at 24 hours after transfection and subjected to Western blot analysis.

Table 1. List of Mission® siRNA ID for siRNA sequences (Sigma Aldrich).

MEF2A #1	SASI_Mm01_00120787
MEF2A #2	SASI_Mm01_00120788
STAT3 #1	SASI_Mm01_00041178
STAT3 #2	SASI_Mm02_00041179

2.11 Luciferase Assay

Transfected cells were washed 3 times with 1X PBS before adding 100 μL of 1X luciferase lysis buffer (20 mM Tris pH 7.4 and 0.1% Triton X-100) to harvest cells by scrapping and collecting into Eppendorf tubes. Tubes were placed in a shaker at for 10 min at 4°C, after which they were spun down in a 4°C microcentrifuge at max speed for 15 min. Once lysed, 20 μL of the cell lysate was transferred to test tubes to measure the enzymatic activity in each sample on a luminometer (Lumat LB, Berthold). Firefly luciferase activity from *MMP9* promoter luciferase gene constructs was measured using the luciferase assay substrate (Promega, #E1501) as per manufacturer instructions and was normalized using the *Renilla* assay substrate (Promega, #E2820). Luciferase activity values obtained were normalized to *Renilla* activity in the same cell extracts and expressed as fold activation to the untreated control or scramble control for siRNA transfections. 10 μg/mL leupeptin and aprotinin, 5 μg/mL pepstatin A, 0.2mM phenylmethylsulfonyl fluoride (PMSF), and 0.5mM sodium orthovanadate was added to the remaining protein lysates after luciferase assay to retain samples for western blot analysis.

2.12 Protein Isolation

Primary cardiomyocytes were harvested for total protein isolation on ice. Cells were washed 3 times with 1X ice-cold PBS. Cells were scrapped and collected with 100 μL of NP-40 lysis buffer (0.5% Nonidet P-40, 50mM Tris-HCl pH 8, 150mM NaCl, 10mM sodium pyrophosphate, 1mM EDTA pH 8, and 0.1M NaF) containing 10 μg/mL leupeptin and aprotinin, 5 μg/mL pepstatin A, 0.2mM phenylmethylsulfonyl fluoride (PMSF), and 0.5mM sodium orthovanadate. Cell lysate was collected into Eppendorf tubes and placed in a shaker for 20 min at

4°C, after which they were spun down in a 4°C microcentrifuge at max speed for 15 min. The supernatant was collected and stored at -80°C until use.

2.13 Bradford Lowry Assay and Protein Sample Preparation

Protein concentrations were determined by a standard Bradford assay using a generated protein standard curve to calculate concentrations of the protein lysate samples. Bovine serum album (BSA, 1 μg/μL) and frozen protein samples were thawed on ice. BSA standards were prepared with increasing concentrations of BSA (0, 2, 4, and 6 μg/μL) and protein lysates were prepared with 1 μL of the sample along with 200 μL of Bradford reagent and ddH_2O until 1000 μL in Eppendorf tubes. The samples were vortexed, spun down and incubated for 5 minutes at room temperature. After incubation, the samples were loaded into plastic cuvettes and the optical density (OD) at 595nm was determined for each sample using a spectrophotometer. A standard curve was generated and used to calculate the protein concentration. Following this, equivalent amounts of protein were denatured in 6X SDS loading buffer (0.28 M Tris-HCl pH 6.8, 30% glycerol, 10% SDS, 0.5 M dithiothreitol, and 0.0012% bromophenol blue) at 100°C for 5 minutes and stored at -20°C until use. 1 μL of 6X SDS loading buffer was used for 5 μg of protein sample.

2.14 Antibodies and Reagents

The following antibody was obtained from Santa Cruz: α-β actin (sc-47778). The following antibodies were obtained from Cell Signaling: α-STAT3 (9139), α-P-STAT3 Tyr705 (9131S). The following antibodies were obtained from Bio-Rad Laboratories: Goat α-mouse IgG-HRP (1706516) and Goat α-rabbit IgG-HRP (1706515). The following antibody was obtained from Abcam: Rabbit MMP9 antibody (ab283575). Rabbit MEF2A polyclonal antibody were produced in house with the assistance of the Animal Care Facility at York University (Toronto, ON, Canada).

2.15 Western Blotting

Protein samples (20-25 μg/well) and 5 μL of pre-stained protein ladder (Bio-Rad, #PM008) were resolved on an SDS-polyacrylamide gel consisting of an 8% or 10% resolving layer (30% acrylamide/Bis solution 35.7:1, 1.5 M Tris-HCl pH 8.8, 10% SDS, 10% ammonium persulfate, ultrapure water, and TEMED) and a 5% stacking layer (30% acrylamide/Bis solution 35.7:1, 1 M Tris-HCl pH6.8, 10% SDS, 10% ammonium persulfate, ultrapure water, and TEMED) with 1X running buffer (24 mM Tris-base, 180 mM glycine, and 3.4mM SDS) at 100V until the dye front reached the bottom. Following this, the proteins were transferred to a methanol activated polyvinylidene difluoride (PVDF) membrane, submerged in transfer buffer (25 mM Tris-base, 192 mM glycine, and 10% methanol). After transferring, the membrane was washed 3 times with 1X Tris-buffered saline containing Tween 20 (TBS-T, 2 mM Tris base, 13.7 mM NaCl, and 0.1% tween 20) and blocked with 5% skim milk in TBST for 90 minutes prior to primary antibody incubation. The membrane was washed again as previously mentioned, before adding the primary antibody for the protein of interest diluted to a ratio of 1:1000 in 1% milk in TBS-T. The membrane was incubated with the primary antibody overnight at 4°C.

The following day, the membrane was washed again (3X for 15 minutes) before it was incubated with the appropriate HRP-conjugated secondary antibody for 90 minutes, which was diluted to a ratio of 1:2000 in 1% milk in TBS-T. The membrane was washed again (3X for 15 minutes) and incubated with the Enhanced Chemiluminescence (ECL) western blotting substrate (Pierce) for 1 minute prior to visualization with the Invitrogen iBright FL1500 Imaging System. The I-Bright Analysis Software (Thermofisher Scientific) was used to determine the intensity signals. For each western blot, the background was subtracted and intensity of the protein of interest and the respective loading control was determined. The intensity of the protein of interest

was divided by the loading control. The mean ± SEM of each treatment condition was graphed. All graphs were generated using GraphPad Prism 8.

2.16 Immunoprecipitation

Non-transfected and 3xFlag-MEF2A transfected PCMs were harvested, and proteins were extracted as previously mentioned in Section 2.12 and 2.13. Immunoprecipitation (IP) was performed using anti-Flag M2 magnetic beads (MilliporeSigma) and ImmunoCruz Optima kit (Santa Cruz Biotechnology) according to the manufacturer's instructions. Eluted proteins were analyzed by Western blotting as described previously in Section 2.14 and 2.15. The above experiment was performed by Amira Moustafa as described previously (Moustafa, *in press*).

The 3xFlag-MEF2A construct was cloned using Gateway technology (life Technology) into pDEST 5′ Triple Flag pCDNA5 FRT TO vector carrying an N-terminal 3xFlag tag and ccdb sequence between attR1 and attR2. PCR product for full-length MEF2A was generated with primers containing attB sites. The PCR reaction was cleaned using Qiagen PCR purification kit (Life Technologies, #28104) and cloned into pDONR223 vector using the BP clones kit (Life Technologies, #11789). The entry clone was recombined into the pDEST 5′ Triple Flag pCDNA5 FRT TO destination vector using the LR clonase kit (Life Technologies, #12538). The resulting vector was verified by DNA sequencing. The above experiment was performed by Amira Moustafa as described previously (Moustafa et al., *in press*).

2.17 Isolation of RNA and Acetone Protein Precipitation

Primary cardiomyocytes were harvested for total RNA isolation on ice. Cells were washed with 1X ice-cold sterile DNase/RNase-free PBS. RNA extraction was carried out using the RNeasy Plus kit (Qiagen, #74104) according to manufacturer's instructions, except that RNA samples were

eluted with 30 µL of RNase free water instead of 50 µL. RNA concentration, absorbance ratio, and 260nm/280nm was measured using a NanoDrop 2000 spectrophotometer. To isolate protein from RLT Buffer lysate flow-through from RNA isolation spin column, 4 volumes of acetone, chilled to -20°C, was added to the flow-through lysate and the mixture was incubated at -80°C overnight. Lysates were then spun down in a 4°C microcentrifuge at max speed for 20 min. The supernatant was discarded, and pellet was left to air-dry. Pellet was re-suspended in 50 µL of 1X luciferase lysis buffer containing 10 µg/mL leupeptin and aprotinin, 5 µg/mL pepstatin A, 0.2mM phenylmethylsulfonyl fluoride (PMSF), and 0.5mM sodium orthovanadate and vortexed until full homogenization. Prior to western blot analysis, protein lysate concentrations were determined by a standard Bradford assay. Following this, equivalent amounts of protein were denatured in 6X SDS loading buffer at 100°C for 5 minutes and immediately loaded on a fresh SDS-PAGE gel for western blot analysis.

2.18 Reverse Transcription (RT) of cDNA From Total RNA

Total RNA isolated from the primary cardiomyocyte was immediately converted to cDNA using the High-Capacity RNA-to-cDNA Kit (Applied Biosystems, #4387406) according to the manufacturer's instructions. 2 µg of RNA was converted to 2 µg of DNA for each experimental condition. DNase/RNase water was used as a negative control. The reverse transcription was performed using the thermocycler and the samples were incubated at 37ºC for 60 minutes, followed by heat inactivation of the RT enzyme 95ºC for 5 minutes and a hold at 4ºC. cDNAs were stored at -20°C until further quantification.

2.19 qPCR Primer Design

All qPCR primers for this project were designed with Primer3 using only the coding region of the gene in the *R. norvegicus* genome and specificity was determined using NCBI Primer Blast.

Primer 3: https://bioinfo.ut.ee/primer3-0.4.0/

NCBI Primer Blast: https://www.ncbi.nlm.nih.gov/tools/primer-blast/

Primer pairs were chosen based on optimal Tm, GC%, self-complementarity and were validated to ensure there were no off-target hits. Forward and Reverse primer sequences can be found in **Table 2**. Primers were selected to be 10-22 bps with amplicon size restricted to 100-150 bps and the melting temperatures were restricted to 58°C to 62°C, with a difference of ±2°C between primer pairs. Acceptable primer GC content was 50 to 60%. Primer pairs were analyzed for possible hairpin structures, self-complementarity, primer-primer interactions, and mismatched annealing. For each gene, two candidate primers were selected and tested.

Table 2. List of forward and reverse primers for RT-qPCR.

β-actin	Fwd: 5' -GGGAAATCGTGCGTGACATTAA- 3' Rev: 5' -TGCCGATAGTGATGACCTGAC- 3'
MEF2A	Fwd: 5' -TGAACAGTCGGAAACCAGATCT- 3' Rev: 5' -AGGTTGTGTGGCTTGAGAACTA- 3'
STAT3	Fwd: 5' -AGTGACTCAAAGCCACCTTACT- 3' Rev: 5' -GTGGTCAAGGCAAGCAGTTT- 3'
MMP9	Fwd: 5' -GATCCGCAGTCCAAGAAGATTT- 3' Rev: 5' -TCTGAGCCTAGACCCAACTTAT- 3'

2.20 qPCR Primer Optimization

The efficiency of candidate primers was determined by conducting a serial qPCR with varying cDNA and primer dilutions. The primers were optimized for BlasTaq 2X qPCR MasterMix (ABM,

#G891), and the assay efficiency was verified by generating a standard curve. First, the cDNA sample of the scrambled control was diluted to 1 in 40. Following this, the 1:40 stock cDNA dilution was diluted further to set up serial dilutions to generate cDNA standards of the following dilution ratios; 1:1, 1:2, 1:4, 1:8, and 1:16. Candidate primer pairs were tested as per **Table 3**. One of the following tables below was utilized for each candidate gene of interest.

Table 3: Primer Optimization Tables.

Table A

Contents	1x
BlasTaq 2X	10 µL
10µM F. Primer	2 µL
10µM R. Primer	2 µL
ddH2O	4 µL
cDNA template	2 µL
Total Volume	20 µL

Table B

Contents	1x
BlasTaq 2X	10 µL
10µM F. Primer	1 µL
10µM R. Primer	1 µL
ddH2O	6 µL
cDNA template	2µL
Total Volume	20 µL

Table C

Contents	1x
BlasTaq 2X	10 µL
10µM F. Primer	0.5 µL
10µM R. Primer	0.5 µL
ddH2O	7 µL
cDNA template	2 µL
Total Volume	20 µL

At each primer concentration, qPCR for the cDNA standards was done. qPCR reactions were run using the Rotor-Gene Q (Qiagen) with the BlasTaq 2X qPCR MasterMix, following the manufacturer's protocol. Parameters for qRT-PCR: enzyme activation at 95^{o}C for 3 minutes, denaturation and extension at [95^{o}C for 15 seconds, 60^{o}C for 1 minute] x 40 cycles. Reactions were run in duplicates, along with negative controls that contained no cDNA. Average Ct values were plotted against the logarithm cDNA standard. The slope of this relationship was used to calculate the primer efficiency (%) as per the equation noted below:

$$Primer\ Efficiency\ (\%) = \left(10^{\frac{-1}{slope}} - 1\right) X\ 100$$

Table 4. qPCR primer optimization using the standard curve.

β-Actin, MEF2A, STAT3 and MMP9 were optimized as per Section 2.19 of the Materials and Methods. Primer efficiency within 98-100% was acceptable for the purposes of this thesis. The candidate primer which passed these tests at their optimization tables (**Table 3**) are highlighted in red and were selected for experiments.

Gene	Table 3A	Table 3B	Table 3C
β-Actin	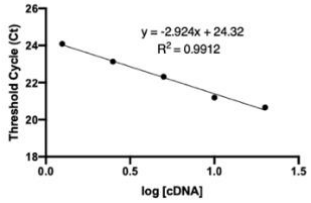	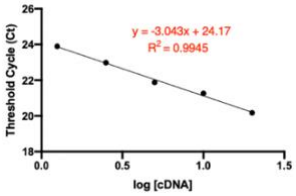	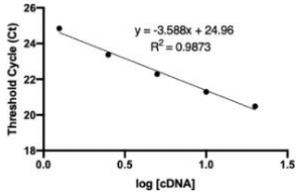
MEF2A	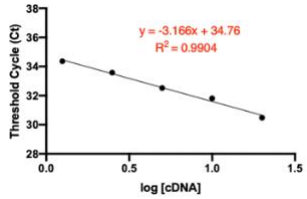	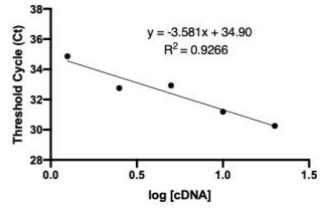	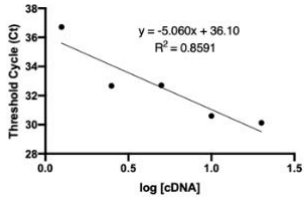
STAT3	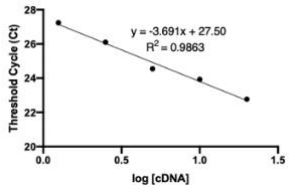	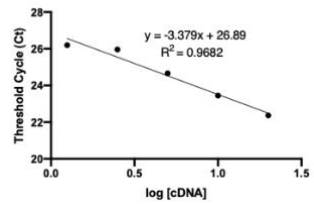	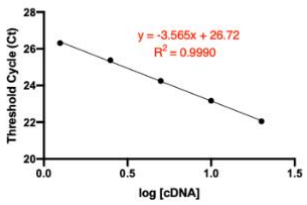
MMP9	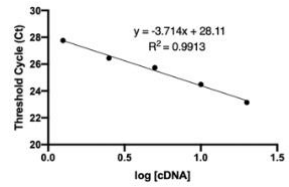	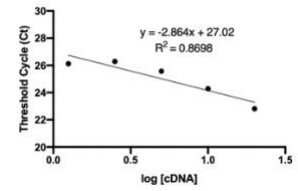	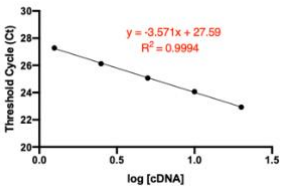

2.21 Quantitative Polymerase Chain Reaction (qPCR)

RT-PCR was carried out using BlasTaq 2X qPCR MasterMix (ABM, #G891), following the manufacturer's protocol. The levels of mRNAs for experimental conditions were normalized to endogenous housekeeping gene β-Actin. Selected Forward and Reverse primer sequences for

genes of interest can be found in **Table 2**. The cDNA was diluted 1:40 prior to use. 2 µl cDNA was mixed with master mix and the optimized primer concentration in a final volume of 20 µl. Each sample was prepared in duplicates and analyzed using Rotor-Gene Q (Qiagen). Parameters for qRT-PCR: enzyme activation at 95ºC for 3 minutes, denaturation and extension at [95ºC for 15 seconds, 60ºC for 1 minute] x 40 cycles. The fold change was quantified using the $2^{-\Delta\Delta Ct}$ method to analyze the data sets and all experimental conditions were normalized to β-Actin. Data was obtained from two independent experiments (N=2) ran in quadruplets.

2.22 Statistical Analysis

All experiments were performed for an N=3 biological replicates, unless stated otherwise (N=2 for RT-qPCR). Data is presented as the MEAN±SEM. One-way analysis of variance followed by a Tukey HSD post hoc test was performed on experiments as all contained greater than two conditions. Differences were considered statistically significant if $p < 0.05$. * is p-value ≤ 0.05, **is p-value ≤ 0.01, *** is p-value ≤ 0.001. All statistical analyses were done using GraphPad Prism 8 with the experimental parameters listed under each figure.

3. RESULTS

The foundation of the experiments contained in this thesis concerning the STAT3:MEF2A complex stem from the interactome and transcriptome experiments conducted by Amira Moustafa in the McDermott lab at York University. The affinity purification experiments coupled with quantitative mass spectrometry proteomics highlighted a biochemical interaction between MEF2A and STAT3 (Moustafa et al., *in press*). The STAT family of transcription factors have important roles in cardio-protection and modulating the transcriptional response to varying physiological and pathological adaptations of the heart (Harhous, Booz, Ovize, Bidaux, & Kurdi, 2019).

As a transcription factor, STAT3 regulates gene transcription by directly modulating gene transcription through its transactivation domain (Sgrignani et al., 2018; Turkson et al., 1998). It is important to mention that STAT3 has a dual function by which it can inhibit, activate or attenuate gene transcription by targeting the promoter regions of specific target genes through the recruitment of a tyrosine phosphatase to inhibit the assembly of the enhanceosome complex (Lerner, Henriksen, Zhang, & Darnell, 2003; Zhuo Wang et al., 2019). Additionally, another level of STAT3 target gene regulation specificity is conferred by the ability of the transcription machinery to recruit co-transcription factors alongside STAT3 to regulate gene transcription (Giraud et al., 2002). The involvement of cis-regulatory elements in gene transcription regulation is crucial. Cooperative actions between STAT3 and co-factors like AP-1 and SP-1 have been heavily investigated and this thesis seek to further to investigate this novel complex with MEF2A (Itoh et al., 2006; Zugowski et al., 2011).

As previously mentioned, Moustafa also conducted experiments that aimed to assess the nature of the MEF2A:STAT3 interaction using a MEF2 luciferase reporter gene assay. The results

confirmed that STAT3 represses MEF2 transactivation function in NRVMs through gain of function (ectopic overexpression), loss of function (siRNA depletion) and pharmacologic inhibition (STAT3 inhibitor XIII, C188-9) experiments on MEF2-luciferase dependent promoter regions. It was concluded that the repressive effect of STAT3 on MEF2 transactivation are more robust than the reciprocal effect of STAT3 on MEF2A. Based on this, it is important to further gauge the potential of this interaction by investigating their resultant effects on a downstream gene like MMP9 that appears to be inversely co-regulated by both MEF2A and STAT3.

3.1 Biochemical Validation of Protein Interaction Between MEF2A and STAT3

For the initial purposes of this thesis, an immunoprecipitation was conducted to assess the biochemical interaction between MEF2A and STAT3. Primary cardiomyocytes from neonatal rats were selected as the model of choice to reflect cardiomyocyte biology most accurately in the cell culture system. **Figure 9A** illustrates the workflow for isolating NRVMs, which was followed by the transfection of a Flag-Tag-3X-MEF2A expression system. The Flag-Tag expression system improves the detection of the chosen recombinant fusion protein, which in this case was MEF2A. Western blot analysis confirmed that the NRVMs were able to successfully overexpress with 3X-Flag-MEF2A and β-actin was used a loading control (**Figure 9B left**).

Cells that were not transfected served as lysates from NRVMs that were the negative control and lysates from NRVMs that overexpressed Flag-MEF2A condition were used for the α-Flag magnetic bead-based immunoprecipitation (**Figure 9B left**). Western blots were conducted using the lysates to assay for α-Flag-Tag, MEF2A, STAT3 and β-actin. The western blots revealed that STAT3 was found in the Flag-MEF2A protein complex, whereas there was no detection of STAT3 in control immunoprecipitation (**Figure 9B center**). The subsequent immunoprecipitation

sought to investigate endogenous interactions between MEF2A and STAT3. The results indicated that an immunoprecipitation of STAT3 also resulted in detection of MEF2A within the eluate, providing evidence of a robust interaction between endogenous MEF2A and STAT3 within the primary cardiomyocytes (**Figure 9B right**).

3.2 Gauging the Impact of MEF2A/STAT3 on MMP9 Promoter and Protein Activity

As previously mentioned, MMP9 was identified as a target of interest following the integrated transcriptome analyses of siRNA-mediated depletion of MEF2A and STAT3 (**Figure 8**). To assess the function of the MEF2A:STAT3 interaction and to interrogate the role of this complex, the effects of STAT3 and MEF2A on the human MMP9 promotor were assessed using the Renilla/Firefly luciferase assay in conjunction with siRNA and pharmacological inhibitors in NRVMs. The human MMP9 promoter (670 bp) driving a firefly luciferase gene was used for evaluation of MMP9 promoter activity. The luciferase driven MMP9 promoter has the reported binding sites for NF-kB, SP-1, AP-1 as confirmed in the literature and non-confirmed binding sites for MEF2A and STAT3 (Takahra, Smart, Oakley, & Mann, 2004).

3.3 Efficiency of siRNA Mediated Gene Silencing for MEF2A and STAT3

The *Renilla* luciferase reporter assay experiments were conducted with human MMP9 luciferase driven promoter using siRNA mediated gene silencing. This would allow for a more direct investigation to interrogate the roles of MEF2A and STAT3 on the same human MMP9 luciferase promoter. The McDermott lab had previously tested two sets of siRNAs for both MEF2A and STAT3 transcription factors that were able to successfully deplete the protein expression level of MEF2A and STAT3. Having this previous data, The NRVMs were transfected

with two sets of siRNAs targeting MEF2A or STAT3 to confirm depletion of the transcription factor of interest (**Figure 10B and 10C)**.

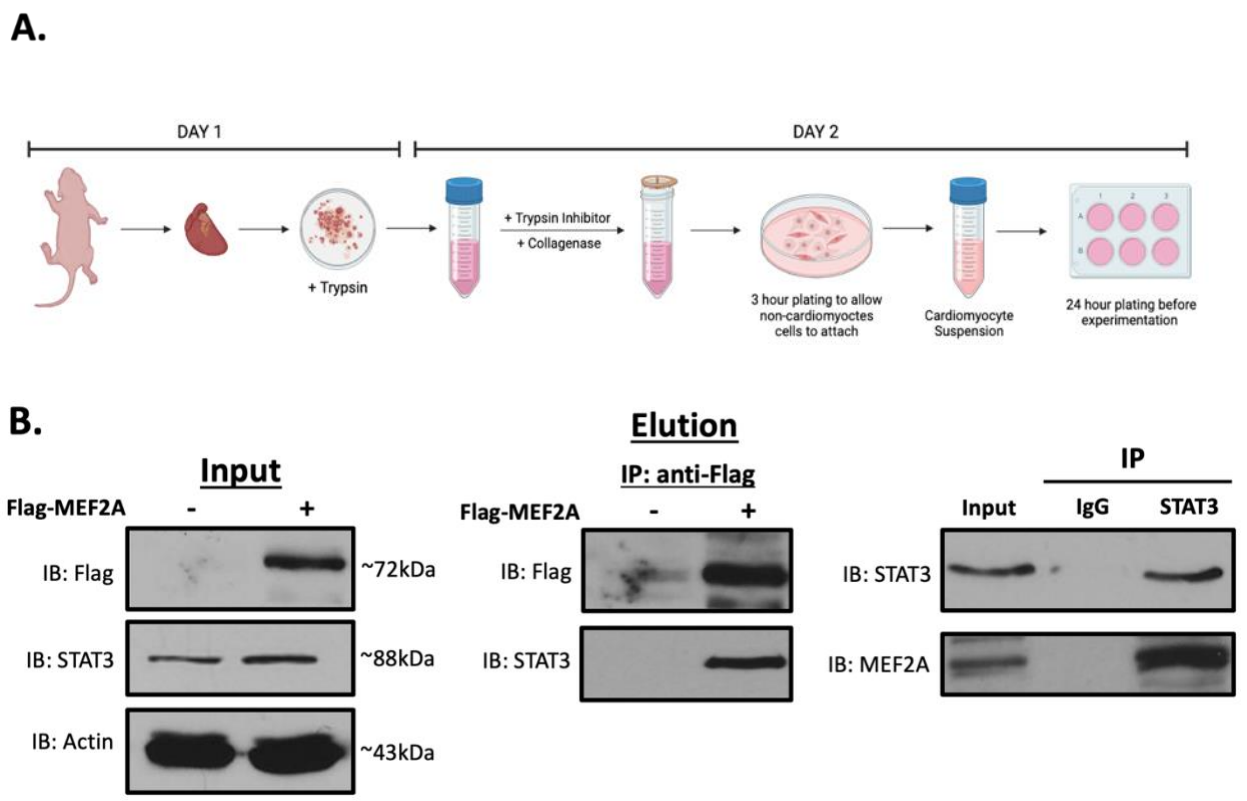

Figure 9: Schematic for NRVM isolation and immunoprecipitation of 3xFLAG-MEF2A and STAT3 interactions.

(A) Primary cardiomyocyte cells were isolated from surgically removed hearts of 1-3 days old rat pups sacrificed by cervical dislocation. The cardiomyocytes were isolated using the Worthington Neonatal Cardiomyocyte Isolation System, see Materials and Methods Sections 2.5 - 2.7 for detailed procedure. **(B)** NRVMs were transfected with a 3xFlag-MEF2A construct and a western blot was conducted using the lysates to assay for Flag-Tag, MEF2A, STAT3 and β-actin. Flag-MEF2A lysates were used for IP using Flag magnetic beads and the eluates were blotted with α-Flag and STAT3 antibodies. IP with lysates from non-transfected NRVMs were used as negative controls with IgG was used as controls. Non-transfected PCM lysates were used for IP using the STAT3 antibody to confirm the interaction between endogenous STAT3 and MEF2A. IP with IgG was used as control (Bottom right). Number of biological replicates carried out for the Western blot and IP data is N=1. Immunoprecipitation western blots were conducted by Amira Moustafa.

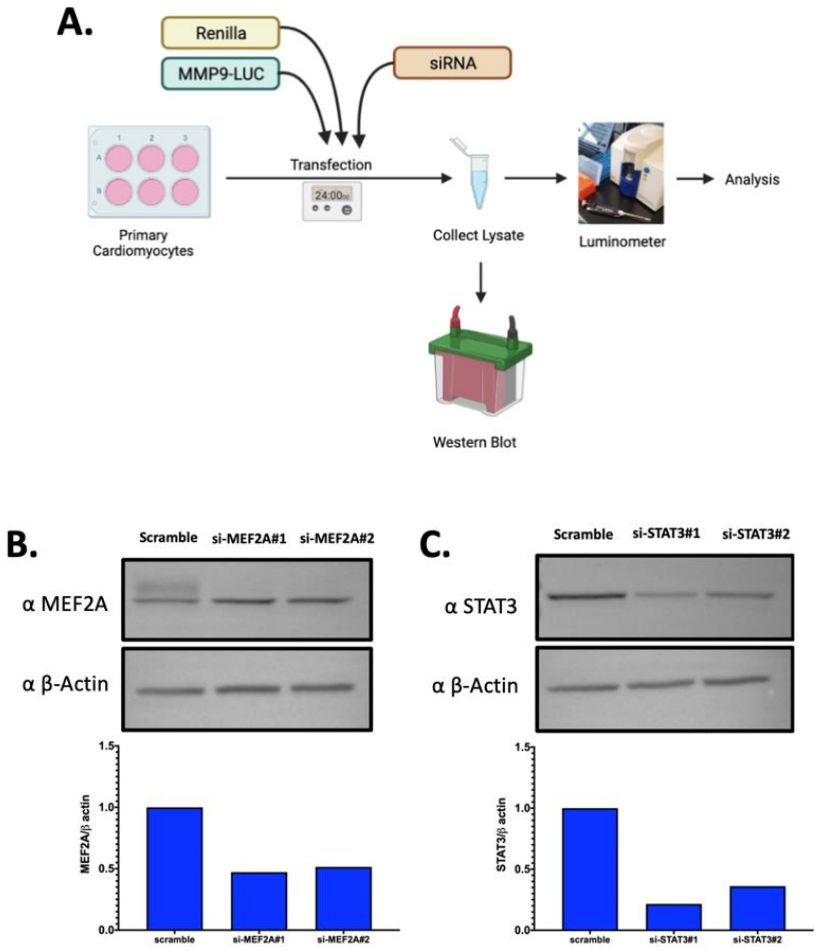

Figure 10: Efficiency of siRNA mediated MEF2A and STAT3 gene silencing in NRVMs.

(A) Primary NRVM cells were co-transfected with siRNA duplexes of universal scrambled control, siMEF2A#1, and siSTAT3#1 with Lipofectamine RNAiMAX; and the *MMP9* firefly luciferase gene reporter plasmid construct and a control pRL-*Renilla* plasmid construct using the Lipofectamine 2000 transfection reagent. 24 hours after transfection cells were harvested for luciferase assay and remaining protein lysates were retained as samples for western blot analysis. **(B)** Two different siRNA (si-MEF2A#1 and si-MEF2A#2) targeting MEF2A were transfected into neonatal rat cardiomyocytes at 200 nM for 24 hours. **(C)** Two different siRNA (si-STAT3#1 and si-STAT3#2) targeting STAT3 were transfected into neonatal rat cardiomyocytes at 200 nM for 24 hours. The relative intensity of the protein bands was first standardized to β-actin (loading control). The data was derived from 1 experiment (N=1), was normalized to the scramble control condition, and plotted in the bar graph.

3.4 STAT3 Depletion Increases Activity of Human-MMP9 Luciferase Promotor

The NRVMs were transfected with the human MMP9 luciferase reporter and a *Renilla* luciferase control. At the same time, the cells were also transfected with either the scrambled siRNA control, siMEF2A#1, siSTAT3#1 or a combinatory siRNA combination of siMEF2A#1 and siSTAT3#1 using RNAiMAX. The control condition was the NRVM cells that were transfected with the scramble siRNA, which should not have any impact on the cells. The firefly luciferase activity under each condition was measured independently and normalized to *Renilla* luciferase values. The relative firefly luciferase levels for all conditions were represented as fold change were normalized to the scramble siRNA condition that was transfected with both constructs (**Figure 11A**). Each condition was compared to the scramble siRNA condition for the three individually transfected samples to determine the fold change.

The siRNA-mediated depletion of STAT3 robustly enhanced the expression of the luciferase gene by approximately 8.5-fold compared to the scramble siRNA condition. This was in-line with the results of a C188-9 treatment that inhibited the activation of the STAT3 transcription factor (**Figure 11A**). Interestingly, the combinatory depletion of both MEF2A and STAT3 indicated a significant difference from the independent depletions of MEF2A and STAT3. This indicated that like the combinatorial treatment of SB203580 and C188-9 (**Figure 12**), the addition of siMEF2A significantly mitigated the robust increase as expected in only the siSTAT3 condition to 6.2-fold. Although not significant, the siRNA mediated depletion of MEF2A marginally decreased the promoter activity by ~0.6x (**Figure 11A**).

3.5 siRNA Mediated Depletion Targets MEF2A and STAT3 in Cardiomyocytes

After analyzing the data from the siRNA mediated depletion *Renilla* luciferase assay experiment, it was important to validate that the depletions of MEF2A and STAT3 were successful. This would allow for confirmation that the observations from the siRNA mediated depletion *Renilla* luciferase assay were a direct result of the depletion effects. As previously mentioned, the McDermott lab had previously tested 4 siRNAs for both MEF2A and STAT3. The siRNA for both transcription factors that had significantly depleted the protein expression levels of both MEF2A and STAT3 in the primary neonatal rat cardiomyocytes was selected. This would also allow for the investigation of the direct impacts of the depletion on the MMP9 protein expression level with western blotting.

Western blotting analysis was used to confirm the depletions. The remaining lysate from the human MMP9 luciferase reporter assay experiment was assessed using western blot analysis from the siRNA scramble, siMEF2A#1, siSTAT3#1, and combinatorial siMEF2A#1 and siSTAT3#1 conditions (**Figure 11B**). To determine whether MEF2A and STAT3 depletion were successful in the relevant condition, the protein expression of total MEF2A and total STAT3 was examined (**Figure 11B**). The relative protein expression levels of MEF2A and STAT3 were estimated by measuring the band intensity. Following this, the relative intensity of the bands was first standardized to β-actin and each set of data was normalized to the scramble siRNA condition (**Figure 11C and 11D**).

The relative protein expression level of total MEF2A was significantly decreased in the siMEF2A and the combination siRNA conditions when compared to the scramble siRNA condition (**Figure 11C**). Similarly, the relative protein expression level of total STAT3 was

significantly decreased in the siSTAT3 and the combination siRNA conditions when compared to the scramble siRNA condition (**Figure 11D**). Collectively, these results indicate that the target siRNAs utilized were able to significantly depletion the expression of their target protein.

3.6 siSTAT3 Mediated Depletion Increases MMP9 Protein Levels

There is great advantage for using siRNA directly assess the function of the MEF2A and STAT3 interaction on MMP9. Following the results from the MMP9 luciferase assay with the siRNA meditated depletion, a western blot was conducted to investigate how the depletions impact the protein expression levels of MMP9 (**Figure 11B**). After confirming that both siRNAs for MEF2A and STAT3 was able to effectively depletion the transcription factors (**Figure 11E**), the results from the MMP9 western blot indicated a significant increase in the protein expression level of MMP9 with the STAT3 depletion when compared to the scramble siRNA condition (**Figure 11E**). Importantly, there was a significant decrease in MMP9 protein expression levels after MEF2A depletion when compared to the scramble siRNA condition (**Figure 11E**).

Most interestingly, there was a significant difference in MMP9 protein expression levels when doing a cross comparison of all the siRNA mediated depletions of MEF2A and STAT3. The combinatorial siRNA-mediated depletion of MEF2A and STAT3 did not result in the significant increase in expression of MMP9 protein levels. This confirms that the combinatorial condition does not allow the significant expression of MMP9 protein as expected in the sole depletion of STAT3, as the depletion of MEF2A prevents a similar increase. Collectively taken, the siRNA-mediated depletion displayed similar effects to that of the C188-9 treatment (**Figure 11 and 12**).

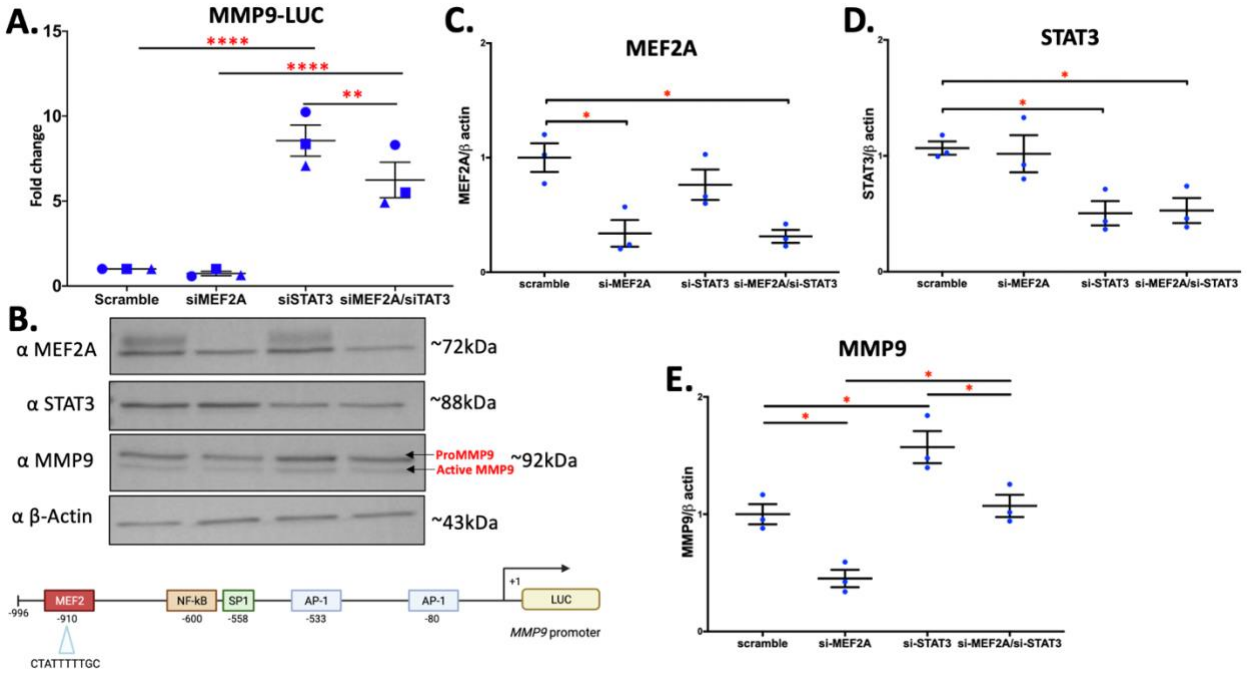

Figure 11: Results of the MMP9-luciferase reporter assay and western blots with siRNA mediated gene silencing of MEF2A and STAT3.

(A) The pRL-*Renilla* plasmid and MMP9 luciferase expression plasmid were transfected into NRVMs alongside the siRNA scramble control, si-MEF2A#1 and si-STAT3#1 according to the four conditions. The firefly luciferase activity under each condition was measured independently and normalized to *Renilla* luciferase values. Each condition is compared to the scramble control for the three individually transfected samples to determine fold change. Each dot or immunoblot represents one biological replicate, corresponding to the mean of 3 technical replicates. **(B)** Western blots of the cell lysates harvested for the reporter assay. Lysates were assessed for the expression of STAT3, MEF2A, MMP9, β-Actin using western blot analysis and visualized with HRP chemiluminescence using the Invitrogen iBright FL1000 imaging system. The relative expression level of STAT3, MEF2A and MMP9 was estimated by measuring the band intensity corresponding to the protein of interest with the iBright analysis software. The relative intensity of the bands was first standardized to β-actin (loading control). **(C, D and E)** The relative expression level of STAT3, MEF2A and MMP9 was estimated by measuring the band intensity corresponding to the protein of interest with the iBright analysis software. The relative intensity of the bands was first standardized to β-actin (loading control). Data in above experiments was derived from 3 independent experiments (N=3) and normalized to the control/scramble condition. The error bars represent standard error of the mean (SEM). Statistical analysis was conducted with the Tukey's multiple comparisons test in one-way ANOVA using GraphPad Prism8; **** $P < 0.0001$, *** $P < 0.001$, ** $P < 0.01$, * $P < 0.05$.

3.7 Pharmacological Inhibition to Target MEF2A and STAT3

Based on the current literature, pharmacological inhibitors SB203580 and C188-9 were selected, respectively targeting MEF2A and STAT3 through different mechanisms. As previously stated, SB203580 inhibits the catalytic activity of p38 MAPK by binding to the ATP-binding pocket, making in an ideal pharmacological target for MEF2A. (Cuenda et al., 1995; Goedert et al., 1997; Kumar et al., 1997; Lee et al., 1994). Similarly, C188-9 is a STAT3 tyrosine 705 inhibitor that has been shown to bind to STAT3 with high affinity and inhibit STAT3 binding to its pY-peptide ligand resulting in a reduction in the constitutive phosphorylated STAT3 activity (Bharadwaj et al., 2016; Kong et al., 2021).

Following the siRNA experiments, inhibitors were used to modulate and further gauge the effect of MEF2A and STAT3 on a common gene target like MMP9. NRVMs were transfected with the human MMP9 firefuly luciferase reporter and a *Renilla* control construct. Following this, transfected cells were treated with either SB203580 or C188-9 and a dual treatment of both inhibitors. To ensure that any effect of the SB203580 treatment was limited to the inhibitor, the cells were also treated with a SB202470, an inactive analog for SB203580. Additionally, the cells were also treated with DMSO, the vehicle control for C188-9. In total, there were 7 conditions for each experiment: Untreated, SB202470, SB203580, DMSO, C188-9, SB202470 and DMSO, SB203580 and C188-9.

The cells in the SB202470 or SB203580 condition were treated for 16 hours, and the cells in the DMSO or C188-9 condition were treated for 1 hour. For the combination treatment conditions, the cells were first treated with either SB202470 or SB203580 for a 16-hour period and followed by a 1-hour treatment of either DMSO or C188-9. The relative firefly luciferase

levels for all conditions represented as fold change were normalized to the untreated control condition, that was transfected with both constructs but was not treated with any pharmacological inhibitors (**Figure 12A**).

3.8 C188-9 Increases Activity of Human-MMP9 Luciferase Promotor

Each experimental condition was compared to the untreated control for the three individually transfected samples to determine the fold change. The inactive analogue, SB202470, and the vehicle carrier control, DMSO, were not significant when compared to the untreated control. Although not significant, SB203580 marginally decreased transcription of the luciferase gene by approximately 0.6-fold when compared to the inactive analogue, SB202470 (**Figure 12A**).

More notably, C188-9 appeared to significantly enhance the expression of the luciferase gene by approximately 3.7-fold in comparison to both the untreated condition and DMSO, the vehicle carrier condition (**Figure 12A**). Interestingly, a combination treatment of C188-9 and SB203580 indicated a significant difference from both the individual treatments of SB203580 and C188-9 indicating that SB203580 treatment in conjunction mitigated the robust increase as expected in the stand-alone C188-9 treatment . The combinatory SB203580 and C188-9 treatments increased the expression of the luciferase gene by approximately 2.8-fold (**Figure 12A**).

3.9 C188-9 Effectively Inhibits the Phosphorylation (Tyr705) of STAT3

Several research groups have successfully identified STAT3 small molecule inhibitors using structure based virtual ligand screens, and cell-based phenotypic screening (Kong et al., 2021). As such, C188-9 was selected as the pharmacological inhibitor to target STAT3, so the effect on MMP9 regulation could be discerned. Western blotting analysis was used confirm that C188-9 is an effective target for the inhibition of STAT3 activation in primary cardiomyocytes.

The remaining lysate from the human MMP9 luciferase reporter assay experiment was assessed using western blot analysis with equal amounts of protein (15 μg) loaded from the 7 conditions (**Figure 12B**). To determine whether C188-9 successfully inhibited STAT3 activation, the protein expression of total STAT3 and phosphorylated STAT3 at Tyr705 (Y705) was examined.

The relative protein expression levels of STAT3 and phosphorylated-STAT3 were estimated by measuring the band intensity. Following this, the relative intensity of the bands was first standardized to β-actin and each set of data was normalized to the untreated condition (**Figure 12C and 12D**). The relative protein expression level of total STAT3 was unchanged in all 7 conditions (**Figure 12C**). However, the relative protein expression level of phosphorylated-STAT3 (Y705) was significantly reduced in the C188-9 and the combination SB203580/C188-9 conditions when compared to their respective vehicle controls of DMSO and SB202470/DMSO (**Figure 12D**). The protein expression level of phosphorylated-STAT3 was not significantly different when comparing the untreated control to the vehicle carrier control of DMSO. Collectively, these results indicate that C188-9 does significantly reduce the phosphorylation of STAT3 (Y705), indicating that it is an ideal target for the inhibition of STAT3 activation in the primary cardiomyocyte cell culture of NRVMs.

3.10 Effect of SB203580 on p38 MAPK, Phosphorylated p38MAPK and MEF2A

It is well documented in that MEF2 is activated through phosphorylation by the p38 MAPK pathway (Yang, Galanis, & Sharrocks, 1999). As such, we selected p38 MAPK inhibitor SB203580 as the pharmacological inhibitor, so the effect of MEF2A on MMP9 regulation could be discerned. Activated p38 MAPK has been shown to phosphorylate and activate MEF2 transcription factors (Raingeaud et al., 1995). The SB203580 inhibitor has been shown to

preferentially bind to the inactive, non-phosphorylated form of p38 MAPK (Zhulun Wang et al., 1998; Young et al., 1997). It is important to note that binding affinity of SB203580 does not differ between the active and inactive forms, whereas ATP binds more weakly to the inactive form, giving SB203580 a significant competitive advantage in its preferential binding to the inactive form of p38MAPK (Young et al., 1997). Most important to note, that although SB203580 inhibits p38MAPK catalytic activity by binding to the ATP-binding pocket, it does not fully inhibit the phosphorylation of p38 MAPK by upstream kinases like MKK3, MKK6, and SEK (Kumar, Jiang, Adams, & Lee, 1999). Following this, it has become reasonable to conclude that SB203580 may "lock" the kinase in an inactive form, significantly reducing the active phosphorylated form of p38 MAPK, although there is still the possibility of phosphorylation of p38 MAPK by the upstream kinases.

Western blotting analysis was used to confirm whether the pharmacological inhibitor SB203580 was able to significantly "lock" the p38 MAPK in its inactive, non-phosphorylated form in comparison to its active phosphorylated form, in addition to any impact on protein levels of MEF2A (**Figure 12F**). Once again, the lysate from the human MMP9 luciferase reporter assay experiment was assessed using western blot analysis with equal amounts of protein (15 μg) loaded from the 7 conditions (**Figure 12B**). First, the protein expression of total p38 MAPK and total phosphorylated p38 MAPK (p-p38) was examined (**Figure 12F, 12G and 12H**). In addition to this, the protein expression of MEF2A was examined to evaluate any significant changes in the protein level. As mentioned, SB203580 is not a direct target for MEF2A, but is a general p38MAPK inhibitor that may impact any p38 MAPK-dependent pathway in the cardiomyocytes. The relative protein expression level of p38 MAPK, phosphorylated-p38 MAPK and MEF2A were estimated by measuring the band intensity. Following this, the relative intensity of the bands was

first standardized to β-actin and each set of data was normalized to the untreated condition (**Figure 12F, 12G, and 12H**). The relative protein expression level of total p38 MAPK and MEF2A was unchanged in all 7 conditions (**Figure 12F and 12G**). However, the relative protein expression level of phosphorylated-p38 MAPK was significantly increased in the SB203580, C188-9 and the combined treatment conditions when compared to inactive analogue SB202470 or DMSO controls specific for each inhibitor (**Figure 12H**).

3.11 MMP9 Protein Level Increases with C188-9 Treatment in NRVMs

As previously mentioned, the main objective of using the pharmacological inhibitors was to assess the function of the MEF2A:STAT3 interaction on MMP9. Based on the results from the *MMP9* luciferase assay with the pharmacological inhibitors, the effects of C188-9, SB203580 and the combined treatment on the protein expression levels of MMP9 were evaluated. After confirming that C188-9 was able to effectively target the activation of STAT3 (**Figure 12A**), the results from the MMP9 western blot indicated a significant increase in the protein expression level of MMP9 for the C188-9 treatment (**Figure 12B**). Importantly, there was no difference in total phosphorylated p38 MAPK and MEF2A protein expression levels after the SB203580 treatment, this was also reflected in the expression levels of MMP9 (**Figure 12E**). There was no significant change when comparing the MMP9 protein expression levels in the SB203590 treatment when compared to the inactive analogue SB202470 and the untreated control. Most interestingly, there was a significant difference when the MMP9 protein expression levels in the single C188-9 treatment to the combined treatment condition. This confirms that the combinatorial treatment does not allow the significant expression of MMP9 protein as expected in the stand-alone C188-9 treatment.

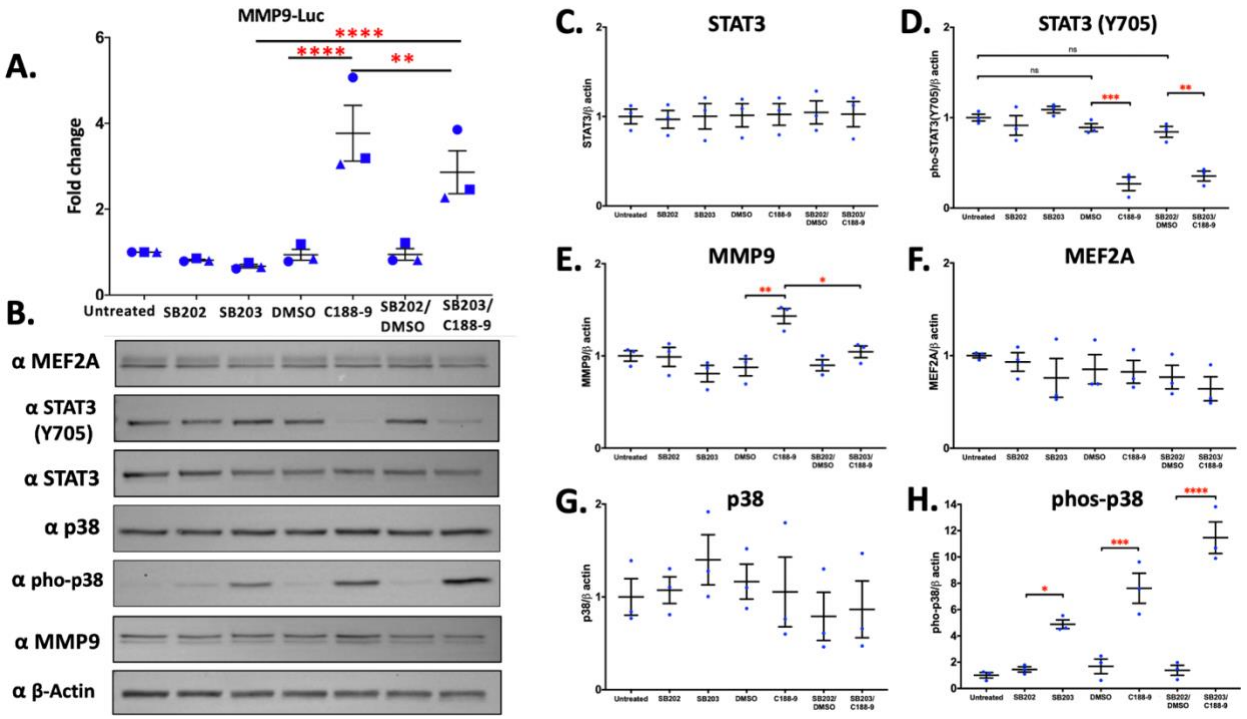

Figure 12: Results of the MMP9-luciferase reporter assay and western blots with the STAT3 inhibitor XIII, C188-9 and the p38 MAPK inhibitor, SB203580.

(A) Results for the Firefly *Renilla* Luciferase reporter assay of the human MMP9 promoter represented as fold change. NRVM cells were isolated from neonatal rats. All cells were co-transfected the pRL-*Renilla* plasmid and the MMP9 luciferase expression plasmid using Lipofectamine2000. After transfection, cells were separated into 7 conditions: Untreated, SB202470 (10μM), SB203580 (10μM), DMSO (10μM), C188-9 (10μM), SB202470 and DMSO, SB203580 and C188-9. The firefly luciferase activity under each condition was measured independently and normalized to *Renilla* luciferase values. Each condition is compared to the untreated control for the three individually transfected samples to determine fold change. Each dot in the reporter assay represents one biological replicate, corresponding to the mean of 3 technical replicates. **(B)** Western blots of the cell lysates harvested for the reporter assay. Lysates were assessed for the expression of MEF2A, STAT3, phos-STAT3, p38MAPK, phos-p38MAPk, MMP9, and β-Actin using western blot analysis and visualized with HRP chemiluminescence using the Invitrogen iBright FL1000 imaging system. **(C, D, E, F, G, H)** The relative expression level of protein was estimated by measuring the band intensity corresponding to the protein of interest with the iBright analysis software. The relative intensity of the bands was first standardized to β-actin (loading control). The data in the above experiments was derived from 3 independent experiments (N=3) and normalized to the untreated condition. The error bars represent standard error of the mean (SEM). Statistical analysis was conducted with the Tukey's multiple comparisons test in one-way ANOVA using GraphPad Prism8; **** $P < 0.0001$, *** $P < 0.001$, ** $P < 0.01$, * $P < 0.05$.

3.12 siMEF2A/siSTAT3 Depletions Target MMP9 Gene Expression at mRNA Level

To validate the siRNA-mediated depletion experiments at the protein level, there was interest in confirming whether the RT-qPCR experiments would yield similar results at the mRNA level. Although it is important to note that changes in protein expression may not fully reflect similarly into changes at the mRNA level. However, if the results aligned, then it would help provide an additional level of confidence that the regulation of MMP9 may be impacted by MEF2A and STAT3 transcription factors at the mRNA level using RT-qPCR. As such, we were interested in not only the MMP9 gene expression, but also the MEF2A and STAT3 gene expression mRNA levels in the siRNA-mediated depletion experiments. NRVMs were transfected with the scrambled siRNA control, siMEF2A#1, siSTAT3#1 or a siRNA combination of siMEF2A#1 and siSTAT3#1 using RNAiMAX (**Figure 13**).

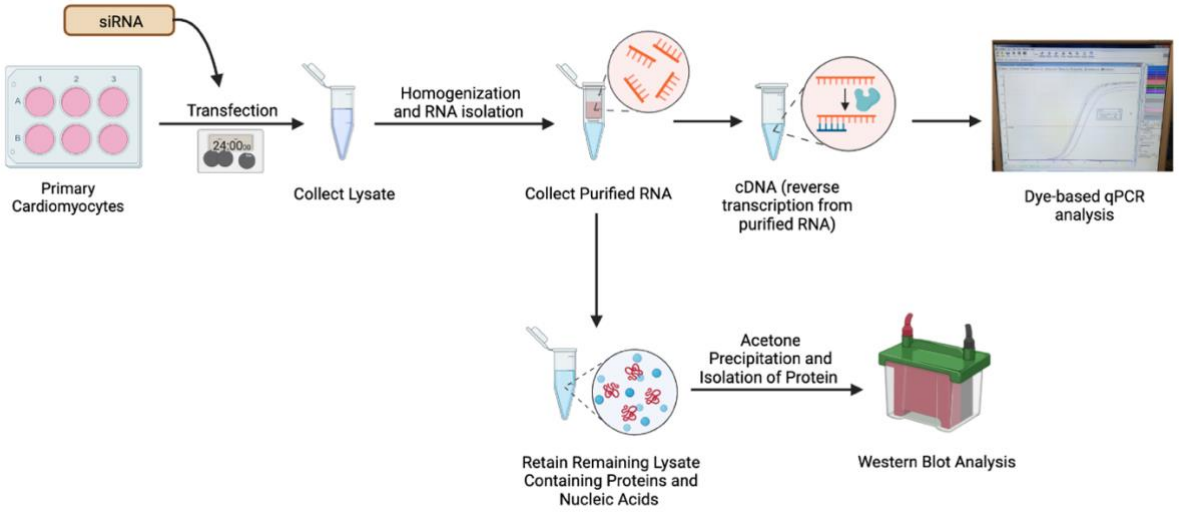

Figure 13: Workflow for RT-qPCR from neonatal rat primary cardiomyocyte culture

Primary cardiomyocyte cells were transfected with siRNA duplexes of universal scrambled control, siMEF2A#1, and siSTAT3#1 with Lipofectamine RNAiMAX. 24 hours after transfection, the cells were harvested for total RNA, protein was precipitated from remaining lysate, followed by cDNA conversion, RT-qPCR, and western blotting.

The control condition were the cells that were transfected with the scrambled siRNA, which should not have any impact on the cells. Following this, primary neonatal cardiomyocyte cells were harvested, and the RNA was isolated using RNeasy Plus Mini Kit and converted to cDNA. The RT-qPCR was performed in duplicates in two separate experimental trials for quadruplets for each independent experiment and acetone precipitation was used to isolate protein lysate for western blot analysis to confirm depletion at the protein level.

The relative mRNA levels for MEF2A, STAT3 and MMP9 for the four siRNA depletion conditions were represented as fold change standardized to β-actin and normalized to the scramble control. To begin, gene expression of MEF2A was analyzed under the four conditions. Although the siRNA-mediated depletion of MEF2A was not significantly decreased from the scrambled control, it was still decreased by approximately half (**Figure 14A**).

Most interesting, it appeared that the the siRNA-mediated depletion of STAT3 enhanced the mRNA expression of MEF2A by approximately 2.3-fold compared to the scramble siRNA condition (**Figure 14A**). This appears to be in line with preliminary data from experiments conducted by Amira Moustafa in which it appeared that STAT3 inhibitor C188-9 appeared to increase MEF2A luciferase reporter activity. This had led to us furthering support that STAT3 exhibits inhibitory effects on MEF2A activity.

Next the gene expression of STAT3 under the four conditions was analyzed. All experimental condition were significantly decreased from the control scramble condition (**Figure 14B**). Most notably, the gene expression of STAT3 was also decreased following the siRNA-mediated depletion of MEF2A. Lastly, we analyzed the gene expression of MMP9 under the four

conditions. The results indicated a significant increase in the protein expression level of MMP9 with the STAT3 depletion when compared to the scramble siRNA condition (**Figure 14C**). Importantly, although there was a decrease in MMP9 protein expression levels by approximately half after MEF2A depletion when compared to the scramble siRNA condition, it was not significant (**Figure 14C**).

There was a significant difference in MMP9 mRNA expression levels when doing a cross comparison of all the siRNA mediated depletions of MEF2A and STAT3. Contrary to previous results of the combinatorial siRNA-mediated depletion of MEF2A and STAT3, the results of this experiment showed a significant increase in expression of MMP9 mRNA levels. Additionally, we used acetone precipitation to isolate protein lysate from the remaining flow-through following the RNA isolation. The purpose of this was to use the lysate to confirm the siRNA-mediated depletions of MEF2A and STAT3 from the siRNA scramble, siMEF2A, siSTAT3, and the dual siMEF2A/siSTAT3#1 conditions (**Figure 14D**).

The relative protein expression level of MEF2A when standardized to β-Actin and normalized to the control were approximately half for the siMEF2A and combination siRNA conditions, when compared to the scrambled control. Similarly, the relative protein expression level of total STAT3 was significantly decreased in the siSTAT3 and the combination siRNA conditions when compared to the scramble siRNA condition. Collectively, these results indicate that the target siRNAs utilized were able to significantly depletion the expression of their target protein for the RNA isolation for RT-qPCR.

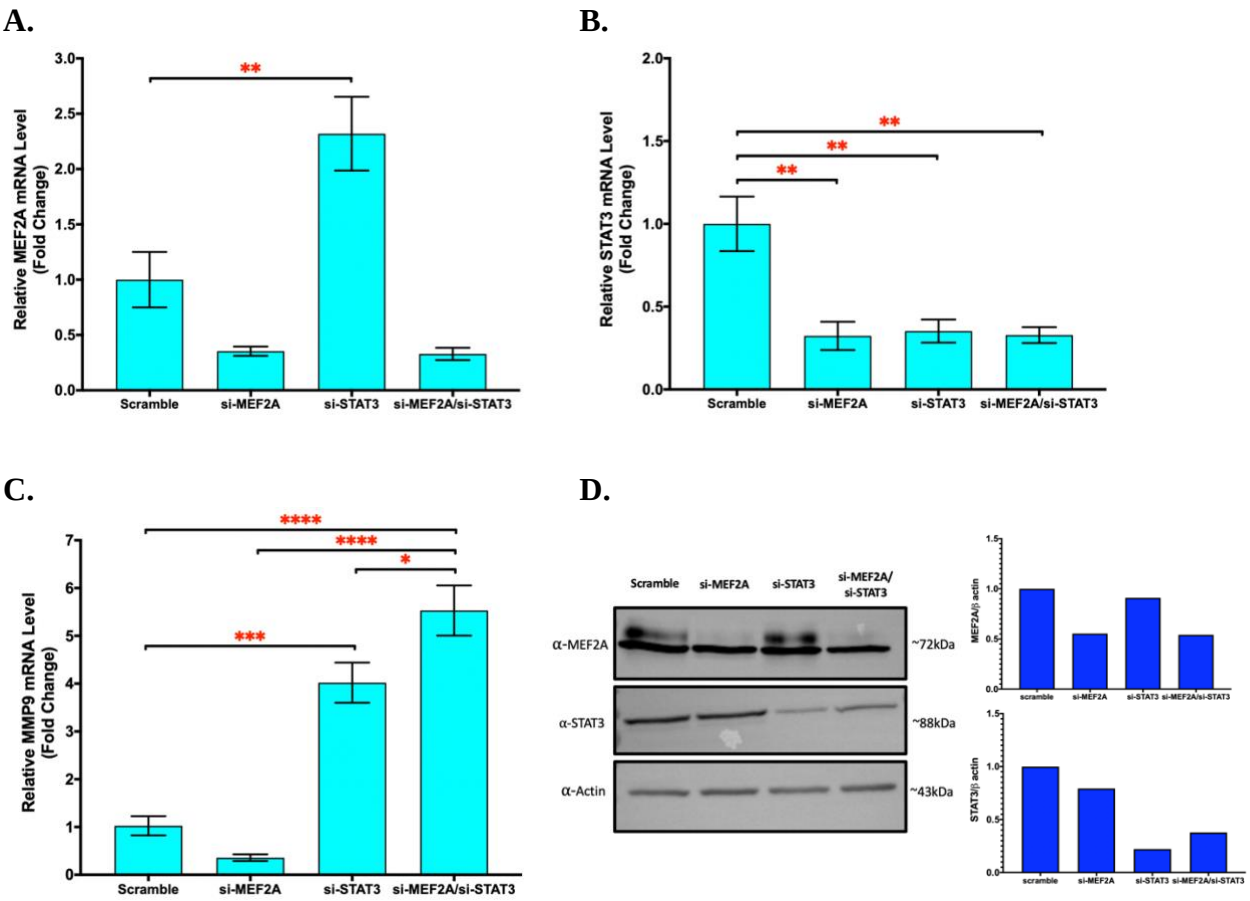

Figure 14: Results of the RT-qPCR and western blots with siRNA mediated gene silencing of MEF2A and STAT3.

Primary cardiomyocyte cells were transfected with siRNA duplexes of scrambled control, siMEF2A#1, and siSTAT3#1 with RNAiMAX. Cells were separated into 4 conditions: siRNA scramble control, siMEF2A, siSTAT3 or a dual siMEF2A+si-STAT3. Total RNAs were isolated, followed by cDNA conversion and RT-qPCR. β-Actin was used as internal control and for standardization of all data sets. (**A**) The relative MEF2A mRNA levels expressed in fold change normalized to scramble control using the $2^{-\Delta\Delta Ct}$ method. (**B**) The relative STAT3 mRNA levels expressed in fold change normalized to scramble control using the $2^{-\Delta\Delta Ct}$ method. (**C**) The relative MMP9 mRNA levels expressed in fold change normalized to scramble control using the $2^{-\Delta\Delta Ct}$ method. The data is derived from 2 independent experiments (N=2), performed in quadruplets and each set of data was normalized to the scramble condition. The error bars represent standard error of the mean (SEM). Statistical analysis was conducted with the Tukey's multiple comparisons test in one-way ANOVA using GraphPad Prism8; **** $P < 0.0001$, *** $P < 0.001$, ** $P < 0.01$, * $P < 0.05$. (**D**) Acetone precipitation of protein was conducted from flow-through lysate following RNA isolation and were assessed for the expression of MEF2A and STAT3 using western blot analysis. The relative expression level of STAT3 and MEF2A was estimated by measuring the band intensity corresponding to the protein of interest with the iBright analysis software. The relative intensity of the bands was standardized to β-actin (loading control). The data was derived from 1 independent experiment (N=1) and was normalized to the scrambled control

4. DISCUSSION

Transcription factors can regulate a multitude of biological processes through their interaction with DNA, interactions with co-factors and through their direct participation in various signalling pathways. The molecular mechanisms with which the MEF2 family of transcription factors can regulate gene expression have been heavily studied in myocytes using in vitro molecular biology techniques such as reporter assays with overexpression. The MEF2 family of transcription factors can repress and activate target genes through interactions with co-factors, which can differ across cell types (Molkentin, Black, Martin, & Olson, 1995; Morin, Charron, Robitaille, & Nemer, 2000).

As previously mentioned, the McDermott lab conducted affinity purification based quantitative proteomics coupled with liquid chromatography tandem mass spectrometry to isolate MEF2A enriched candidate protein-protein associations. Following this, bioinformatic and proteomic analyses with the Qiagen Ingenuity Pathway Analysis software and the Cytoscape software revealed several novel candidate protein-protein associations involving MEF2A. An association between the MEF2A and STAT3 transcription factors was of particular interest as both proteins exert a high level of executive control over many biological processes in neonatal rat ventricular cardiomyocytes (Moustafa et al., *in press*). Currently, it is well-known that MEF2A is a key regulator of cardiac functioning in the developing heart, differentiation, cardiac hypertrophy, heart failure and stress-related cardiac pro-survival response (Black & Olson, 1998; McKinsey et al., 2002; Medrano & Naya, 2017; Olson, 2006; Wales et al., 2014).

Similarly, STAT3 is important for regulating several cardioprotective genes involved in inflammation-based responses, including the innate immune response, the regulation of the

adaptive immune response, and in the defense mechanism and response to cytokines. Additionally, a growing body of evidence has shown that STAT3 is likely to be a key modulator within integrated signalling networks that comprises of different cell types within the heart including cardiomyocytes, inflammatory cells, endothelial cells, fibroblasts, and cardiac progenitor cells (Brutsaert, Fransen, Andries, De Keulenaer, & Sys, 1998; Haghikia, Stapel, Hoch, & Hilfiker-Kleiner, 2011; Harada et al., 2005; Harhous et al., 2019; Osugi et al., 2002; Sgrignani et al., 2018; Zouein, Kurdi, & Booz, 2013).

The association of both MEF2A and STAT3 as a potential complex is of great interest due to their interplay in cardiac transcriptional regulatory networks involved in the pro-survival cellular processes, cardiac hypertrophy, and cell stress-related inflammation responses (Harhous et al., 2019; Hashemi, Salma, et al., 2015; Tobin et al., 2017; Wales et al., 2014). Following the proteomic analyses, the McDermott lab sought to further characterize the MEF2A and STAT3 association using molecular biology and additional bioinformatic techniques. As previously mentioned, siRNA technology was used to generate RNA transcriptomes that integrated NRVM gene targets of interests upon siRNA-mediated depletion of MEF2A and STAT3. This integrated comparative analysis allowed for the identification of common gene regulatory targets or mechanisms that appear to be co-regulated by both MEF2A and STAT3. Through this, MMP9 was identified as one of four potential genes of interest that appeared to show strong evidence for an upregulation through the STAT3 depletion and downregulation through the MEF2A depletion.

4.1 Summary of Findings

With the information available in the literature, taken together with the novel findings of the McDermott Lab, the primary focus on this thesis was to interrogate the MEF2A:STAT3

protein-protein interaction by investigating their regulation of the MMP9 gene at the mRNA, protein expression and luciferase promoter activity levels. As previously stated, the primary hypothesis was that a protein-protein interaction between MEF2A and STAT3 regulates MMP9 gene expression in NRVMs. **Table 5** summarizes key results from all molecular experiments conducted in results section of this thesis. Following the written summary of key results, the remainder of this discussion section will discuss the results with respect to established knowledge within the scientific literature and address new insights where appropriate

Table 5. Summary of the MMP9 molecular biology experiments conducted with NRVMs.

NRVM Condition	**MMP9-luc Promoter Activity**	**MMP9 Protein Expression**	**Relative MMP9 mRNA Levels**
si-MEF2A	no effect	decrease	decrease
si-STAT3	increase	increase	increase
SB203580	no effect	no effect	N/A
C188-9	increase	increase	N/A

To analyze the changes in the MMP9 gene activity using a luciferase driven MMP9 promoter, the STAT3 activity was manipulated using a STAT3 tyrosine 705 inhibitor (C188-9) and the MEF2A activity was targeted with a p38 MAP kinase inhibitor (SB203580). Although reporter gene assays are typically conducted in HEK 293 cells due to ease of growth and transfection, for this thesis, they were conducted the reporter assays in NRVMs to accurately represent the changes in a cellular environment and broaden the application of the results to a cardiac-specific context.

Isolated cardiomyocytes from neonatal and adult rats provide valuable insight into cardiac physiology. It is important to clarify that the rate of protein turnover is tightly regulated for a wide range of transcription factors and signalling proteins that vary from each diverse cell type. There are changes that impact downstream protein stabilization and subsequent accumulation in response to cell signaling events, cellular stress conditions and activation of transcriptional events (Louch, Sheehan, & Wolska, 2011). Although cardiac cell lines such as HL-1 are commercially available, primary isolation and plating of cardiomyocytes is the preferred model and can provide additional data that preserve the *in-vivo* integrity and function of the cells (Claycomb & Palazzo, 1980).

The evidence in the reporter assay experiments in **Figure 11** and **Figure 12** suggest that a potent effect of STAT3 repression through C188-9 leads to a hyperactivation of the MMP9 promoter. Likewise, a more marginal effect of MEF2A is noted on the MMP9 promoter through the p38 MAP kinase inhibitor treatment; SB203580, and MEF2A siRNA depletion. Similarly, STAT3 and MEF2A were depleted with siRNA technology to further interrogate the results of the MMP9 promoter activity using the luciferase reporter gene assay system. It is documented that a STAT3 siRNA depletion and manipulation with C188-9 results in a significant increase in MMP9 luciferase promoter activity levels.

Additionally, due to the results obtained previously using the MEF2 luciferase reporter gene assay experiments, it was important to investigate the impact of a combinatorial depletion or inhibition of both MEF2A and STAT3. In those experiments, it was confirmed that the repressive effect of STAT3 on MEF2 *trans*activation must also be considered. As such, a combined siRNA-mediated depletion of both MEF2A and STAT3 was conducted, in addition to a combined inhibitory dual treatment of SB203580 and C188-9. These data mostly confirmed that there is a

very strong regulation of MMP9 gene expression by manipulation of STAT3 levels or activity and a much weaker influence of MEF2A on this target gene.

Following the MMP9 luciferase reporter gene data analysis, it was important to confirm whether these observations were mirrored at the protein level of MMP9 (**Figure 11B and Figure 12B**). It was confirmed that manipulating STAT3 by depletion with the siRNA or pharmacological inhibition of its activity promotes a corresponding increase in MMP9 protein level which is consistent with the NRVM transcriptome data. The depletion of MEF2A had a marginal effect on MMP9 protein levels, but only with the siRNA based MEF2A depletion.

Lastly, it was investigated whether a depletion of MEF2A, STAT3 or a combined depletion could modulate MMP9 mRNA levels using RT-qPCR (**Figure 14**). When siMEF2A was used, the depletion resulted in a significant decrease in MMP9 mRNA, suggesting that MEF2A could be a potential positive regulator of MMP9 in NRVMs. Additionally, the siSTAT3 mediated depletion resulted in a significant increase in MMP9 mRNA, suggesting that STAT3 could be a potential negative regulator of MMP9 in NRVMs. The data presented here from reporter gene assays, RT-qPCR and protein expression experiments are consistent with the integrated NRVM transcriptome data analysis highlighted in **Figure 8.** Data presented here has identified that MMP9 gene activity is potently regulated by STAT3 and according to the analysis, shows a marginal regulation by MEF2A. Most notably, the interaction between MEF2A and STAT3 is important to consider due to the repressive effects between the two transcription factors and their combined impact on downstream targets such as MMP9.

4.2 Regulation of MMP9 by STAT3

Matrix metalloproteinase-9 (MMP9) is an extracellular endopeptidase that has been extensively studied and is crucial in furthering our understanding of myocardial infarction-related mortality, ventricular remodeling, and cardiac dysfunction (Becirovic-Agic et al., 2021; Kelly et al., 2007; X. Wang & Khalil, 2018). MMP9 is tightly regulated at the transcriptional level by various transcription factors, cytokines, and growth factors (Fanjul-Fernández, Folgueras, Cabrera, & López-Otín, 2010). The promoter region of the human MMP9 gene has multiple functional cis-regulatory regions, including well characterized binding sites for nuclear factor-kB (NF-kB), activator protein-1 (AP-1), and specificity protein-1 (SP-1) (Ma, Shah, Chang, & Benveniste, 2004; Van den Steen et al., 2002; Yan & Boyd, 2007). This combinatorial transcription factor control facilitates recruitment of chromatin remodeling complexes, coactivators, and general transcriptional machinery to activate or repress MMP9 expression within different cell types. Similarly, epigenetic mechanisms such as histone modification, DNA methylation and non-coding RNAs are also important for the transcriptional regulation of MMP9.

In addition to the known transcription factors that influence MMP9 gene transcription, the STAT proteins have a studied relationship with the matrix metalloproteinase families (Spinale, 2007). Previous work has shown that STAT factors translocate to the nucleus following tyrosine phosphorylation (Li, 2008). The tyrosine phosphorylated STAT3 molecule form dimers and bind directly to DNA (Becker, Corthals, Aebersold, Groner, & Müller, 1998). Through this mechanism, the STAT3 factors can regulate the expression of genes that control cell proliferation, differentiation, and apoptosis. More notably, there is also evidence that the stimulation of the STAT pathway is an additional mechanism for increasing the transcription of MMPs in various pathological conditions (Halade, Jin, & Lindsey, 2013).

The evidence presented here documents how MMP9 transcriptional regulation is significantly impacted by STAT3. Data indicates that STAT3 depletion and pharmacological inhibition with C188-9 increases MMP9 promoter activity, protein expression and mRNA levels. These results are supported by studies in the literature that have investigated the effect of STAT3 on MMP9, specifically in cardiomyocytes (Harhous et al., 2019). Furthermore, STAT3 is an important contributor to collagen synthesis and cardiac fibrosis through its activity in cardiac fibroblasts as well as cardiomyocytes (Kurdi, Zgheib, & Booz, 2018; Patel, Nassal, Gratz, & Hund, 2021).

It is also associated with a fibrotic extracellular matrix that has the potential to induce progressive cardiac failure (Haghikia, Ricke-Hoch, Stapel, Gorst, & Hilfiker-Kleiner, 2014; Harhous et al., 2019; Jacoby et al., 2003). STAT3 deletions in mouse cardiomyocytes induce the development of cardiac fibrosis. In diabetic cardiomyopathy contexts, STAT3 has been directed linked to fibrosis that is associated with increased MMP9 expression (Wang et al., 2014). It was also confirmed that STAT3 can directly regulate MMP9 expression in diabetic rats and the suppression of STAT3 inhibited STAT3-mediated cardiac fibrosis through an increase in MMP9 expression (Lo et al., 2017).

An immunoprecipitation assay conducted by Song et al., 2008 demonstrated that the activation of MMP9 promoter is dependent upon interactions of Fra-1/c-Jun with STAT3. This study confirmed the existence of a STAT binding site on the MMP9 promoter in conjunction with the AP-1 site. A complex composed of c-Jun/Fra-1 and STAT3 proteins has been shown to bind the promoter-proximal AP-1 site of the MMP9 gene. This complex appears to play a crucial role in enhanceosome modulation in the activation of MMP9 gene. As such, it has been proven that a

functional cooperation of the STAT3 and AP-1 factors is required for the transcriptional activation of the MMP9 gene (Song et al., 2008).

Although MMP9 upregulation has been strongly tied to an increase in STAT3 proteins in pathological conditions such as cancer, the activation of the STAT proteins does not always induce MMP9 gene expression. Work by Zhao et al., 2007, indicated that MMP9 expression also appears to be repressed because of a potential sequestration of co-activators, such as CBP/p300, by the STAT proteins. This increase in the STAT proteins impairs the direct binding of known MMP9 transcriptional activators such as CBP/p300 to cis-elements on the promoter, resulting in transcriptional reduction of MMP9 (Zhao, Nozell, Ma, & Benveniste, 2007).

STAT3 is known to positively regulate the expression of anti-apoptotic and anti-oxidative proteins, highlighting its cardioprotective role (Harhous et al., 2019). Using a cardiomyocyte specific Cre/lox STAT3 ablation mouse model, Enomoto et al., 2015, reported that STAT3 expression in cardiac myocytes contributes to fibrotic remodeling due to myocardial infarctions (MI). The results of the Enomoto study paralleled our observations reported here. Following an MI in mice with STAT3 ablation, the MMP9 expression and activity was increased (Enomoto et al., 2015). Likewise, we observed that STAT3 depletion resulted in a significant increase in MMP9 promoter activity, mRNA, and protein expression.

As such, the data presented here contribute further evidence supporting the transcriptional regulation of MMP9 by STAT3 in neonatal cardiomyocytes. There is a complex interplay that needs to be considered when investigating the roles of these factors in cardiac pathologies when considering therapeutic potentials or establishing MMP9 as a biomarker for cardiovascular disease (Medeiros et al., 2019).

4.3 Regulation of MMP9 by MEF2A

Although the epigenetic control of matrix metalloproteinase gene expression through the MEF2 factors is understudied, emerging evidence suggests that chromatin remodeling is one mechanism of gene transcription regulation. Chang et al., 2006 have demonstrated that the MEF2 transcription factor is capable of recruiting HDAC5 and/or HDAC7 to the MEF2 binding site in the mouse MMP10 promoter. This interaction results in a significant repression of the expression of MMP10 transcription (Chang et al., 2006). An analysis of the human MMP9 promoter on the eukaryotic promoter database has revealed two MEF2A consensus binding sites on the promoter. Even though the regulation of MMP9 by MEF2A is not extensively studied as evidenced in the literature, there is support for our observations that MMP9 expression decreases due to MEF2A depletion.

Most interestingly, a study conducted by He et al., 2011, showed that aldosterone increased MMP9 activity in cultured neonatal cardiomyocytes, an effect that was dependent on CaMKII activity. Additional DNA sequencing analysis in the study revealed a putative A/T–rich element binding site for MEF2A that was located approximately 670bp upstream of the MMP9 transcription start site. Using wildtype or mutated versions of an MMP9–luciferase reporter constructs to assess the impact of MEF2 on downstream MMP9 promoter activity, the results indicated that mutating the MEF2 binding site significantly decreased MMP9 promoter activity compared to wildtype. Further analyses with MEF2A-lacZ transgenic mice confirmed a hypothesized model of the mechanism through which aldosterone driven cardiac rupture required cardiac MEF2A. These data indicate that the MEF2A-binding site is crucial for aldosterone's increase of MMP9 transcription, which was associated with the cardiac rupture (He et al., 2011)

The observations in this thesis are congruent with the results presented here, highlighting a role for MEF2 in MMP9 regulation. It is important to note that MMP9 is not viewed as a typical canonical target of MEF2A activity as most downstream effector targets are often associated with myogenic differentiation, development, and cardiomyocyte hypertrophy (Naya et al., 1999). Taken together, it can be concluded that MEF2A likely does impact downstream MMP9 transcription activity. MEF2A depletion resulted in a marginal decrease in MMP9 promoter activity and mRNA level. This decrease in MMP9 with MEF2 attenuation is mirrored in the study by He et al., in which they used mutated versions of an MMP9–luciferase reporter construct (He et al., 2011). As such, this is an idea that requires further investigation to uncover additional roles of MEF2 that could be related to cardiac rupture surrounding due to increases in MMP9.

4.4 Interactions between MEF2 And STAT3: Myogenic Differentiation and JAK-STAT

The MEF2A and STAT3 transcription factors have both been shown to have similar regulatory effects for cardiac-specific gene expression. Although the establishment of a physical and functional interaction between both transcription factors is novel (Moustafa et al., *in press*), the literature has alluded to an interplay between both factors due to their involvement in myocyte differentiation, cardiac gene reprogramming and pathological conditions involving cardiac hypertrophy and dysfunction.

It is well-established that myogenic differentiation is critically dependent on the MRF and MEF2 families of transcription factors as they physically interact to activate muscle-specific gene targets (Molkentin et al., 1995). Additionally, MyoD and MEF2 are known to be involved in Myogenin induction at the beginning of differentiation (Edmondson et al., 1994). The direct

binding of MyoD to MEF2 enhances MEF2-dependent transcription and MyoD-dependent transcription through cooperative enhancement during differentiation (Molkentin et al., 1995).

Interestingly, STAT3 was one of the first molecules of the to be implicated in myoblast proliferation in C2C12 cells, due to physically interacting with MyoD (Kataoka et al., 2003; Spangenburg & Booth, 2002). Furthermore, a study conducted by Sun et al., 2007 also provided evidence that the JAK1/STAT1/STAT3 pathway is involved in myoblast proliferation because of its involvement in regulating the expression of p21Cip1, p27Kip1, and Id1. Most interestingly, the JAK1/STAT1/STAT3 pathway also prevented myoblasts from premature differentiation by actively repressing genes like MyoD, MEF2, and Myogenin that are essential for differentiation (Sun et al., 2007). Additional experimental work has also confirmed that STAT3 inhibits myogenic differentiation that is typically induced by low serum conditions as it also induces the expression of c-myc and reciprocally antagonizes MyoD (Kataoka et al., 2003). Similarly, it was shown that STAT3 inhibited not only DNA binding activities of MyoD but also its transcriptional activities (Kataoka et al., 2003).

Previous work in our group has shown that STAT3 does exert a robust repressive effect on MEF2A activity compared to a less reciprocal effect of MEF2A on STAT3 activity (Moustafa et al., *in press*). Additionally, a depletion of both molecules is also linked to a reduction in cell viability. This observation is paralleling the experimental results in the literature and adds evidence to the interaction between MEF2A and STAT3. In this thesis, we confirmed this interaction through immunoprecipitation and illustrated the repressive actions of STAT3 mRNA on MEF2A mRNA levels through the RT-qPCR. As such, it appears that MEF2 and STAT3 appear to co-

regulate genes like MMP9 that are strongly tied to the regulation of cell survival and inflammatory responses (Moustafa et al., *in press*).

Based on the experimental evidence in this thesis, we have proposed a novel model that features a MEF2A and STAT3 negative feedback loop, which also has implications for MMP9 regulation in primary cardiomyocyte cells (**Figure 15**). The physiological relevance of this relationship suggests that MEF2A is an important transcriptional activator of the MMP9 promoter. In fact, the repressive action of STAT3 on the MEF2A transcription factor suggest a degree of control that needs to be further investigated. The physiological importance of MMP9 regulation cannot be underestimated, as plasma levels of MMP9 have been shown to correlate with MI mortality, pathological remodelling of the left ventricle and cardiac dysfunction (Becirovic-Agic et al., 2021; Kelly et al., 2007; Squire et al., 2004).

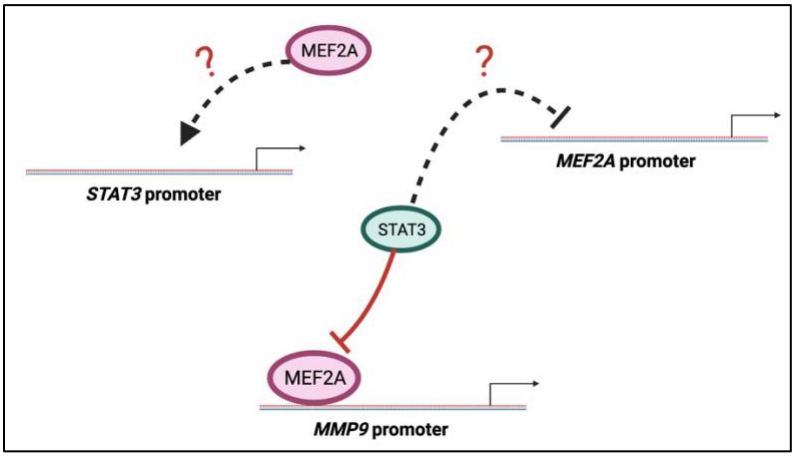

Figure 15: Proposed model of MEF2A/STAT3 negative feedback loop and MMP9 regulation.

4.5 Concluding Remarks and Future Directions

Herein, I present several lines of evidence documenting that MMP9 gene expression is regulated by a novel protein:protein interaction between MEF2A and STAT3 transcription factors

in neonatal rat ventricular cardiomyocytes. Using reporter gene assays, western blot analysis and RT-qPCR, we were able to confirm the preliminary data from the integrated MEF2A and STAT3 transcriptomes. MMP9 activity and expression was upregulated by STAT3 depletion and C188-9 inhibitor treatment, and marginally downregulated by the MEF2A depletion. However, a combined depletion furthered the potential ability to gauge the complex interplay between MEF2A and STAT3 upon depletion of both molecules, highlighting their importance for cell viability. Additionally, we assessed the biochemical interaction between MEF2A and STAT3 using immunoprecipitation. The results revealed that STAT3 was found in the Flag-MEF2A protein complex and immunoprecipitation of STAT3 also resulted in detection of MEF2A. This provides evidence of a robust interaction between endogenous MEF2A and STAT3 in NRVMs.

Further study of the MEF2A and STAT3 protein:protein interaction on three other co-regulated genes; C-X3-C Motif Chemokine Ligand 1 (CX3CL1), C-X-C Motif Chemokine Ligand 10 (CXCL10), lysozyme 2 (LYZ2) is warranted since they are also tied to the innate immune response and have documented involvement of STAT3 (Prabhu & Frangogiannis, 2016). This will allow for a further characterization of the functions of the specific genes with the potential for understanding their roles in cardiac failure and inflammatory infiltration alongside MEF2 and STAT3. Currently, the knowledge of the interaction between MEF2A and STAT3 is still incomplete, and we also propose to further characterize the molecular nature of the interaction in cardiomyocytes. This will no doubt have important implications for our understanding of the therapeutic targets of cardiac immune response and provide more nuanced insights into the etiology of pathological cardiac conditions.

5. REFERENCES

Abu-Issa, R., & Kirby, M. L. (2007). Heart field: from mesoderm to heart tube. *Annu. Rev. Cell Dev. Biol.*, *23*, 45–68.

Backs, J., & Olson, E. N. (2006). Control of cardiac growth by histone acetylation/deacetylation. *Circulation Research*, *98*(1), 15–24.

Becirovic-Agic, M., Chalise, U., Daseke, M. J., Konfrst, S., Salomon, J. D., Mishra, P. K., & Lindsey, M. L. (2021). Infarct in the heart: what's MMP-9 got to do with it? *Biomolecules*, *11*(4), 491.

Becker, S., Corthals, G. L., Aebersold, R., Groner, B., & Müller, C. W. (1998). Expression of a tyrosine phosphorylated, DNA binding Stat3β dimer in bacteria. *FEBS Letters*, *441*(1), 141–147.

Bharadwaj, U., Eckols, T. K., Xu, X., Kasembeli, M. M., Chen, Y., Adachi, M., … Tweardy, D. J. (2016). Small-molecule inhibition of STAT3 in radioresistant head and neck squamous cell carcinoma. *Oncotarget*, *7*(18), 26307.

Black, B., & Cripps, R. (2010). Myocyte Enhancer Factor 2 Transcription Factors in Heart Development and Disease. *Heart Development and Regeneration*, 673–699. https://doi.org/10.1016/B978-0-12-381332-9.00030-X

Black, B. L., & Olson, E. N. (1998). Transcriptional Control of Muscle Development By Myocyte Enhancer Factor-2 (Mef2) Proteins. *Annual Review of Cell and Developmental Biology*, *14*(1), 167–196. https://doi.org/10.1146/annurev.cellbio.14.1.167

Blais, A., Tsikitis, M., Acosta-Alvear, D., Sharan, R., Kluger, Y., & Dynlacht, B. D. (2005). An initial blueprint for myogenic differentiation. *Genes & Development*, *19*(5), 553–569.

Brutsaert, D. L., Fransen, P., Andries, L. J., De Keulenaer, G. W., & Sys, S. U. (1998). Cardiac endothelium and myocardial function. *Cardiovascular Research*, *38*(2), 281–290.

Chang, S., Young, B. D., Li, S., Qi, X., Richardson, J. A., & Olson, E. N. (2006). Histone deacetylase 7 maintains vascular integrity by repressing matrix metalloproteinase 10. *Cell*, *126*(2), 321–334.

Cinghu, S., Yang, P., Kosak, J. P., Conway, A. E., Kumar, D., Oldfield, A. J., … Jothi, R. (2017). Intragenic Enhancers Attenuate Host Gene Expression. *Molecular Cell*, *68*(1), 104-117.e6. https://doi.org/10.1016/j.molcel.2017.09.010

Claycomb, W. C., & Palazzo, M. C. (1980). Culture of the terminally differentiated adult cardiac muscle cell: a light and scanning electron microscope study. *Developmental Biology*, *80*(2), 466–482.

Cuenda, A., Rouse, J., Doza, Y. N., Meier, R., Cohen, P., Gallagher, T. F., … Lee, J. C. (1995). SB 203580 is a specific inhibitor of a MAP kinase homologue which is stimulated by cellular stresses and interleukin-1. *FEBS Letters*, *364*(2), 229–233.

Desjardins, C., & Naya, F. (2016). The Function of the MEF2 Family of Transcription Factors in Cardiac Development, Cardiogenomics, and Direct Reprogramming. *Journal of*

Cardiovascular Development and Disease, *3*(3), 26. https://doi.org/10.3390/jcdd3030026

Dror, I., Golan, T., Levy, C., Rohs, R., & Mandel-Gutfreund, Y. (2015). A widespread role of the motif environment in transcription factor binding across diverse protein families. *Genome Research*, *25*(9), 1268–1280. https://doi.org/10.1101/gr.184671.114

Edmondson, D. G., Lyons, G. E., Martin, J. F., & Olson, E. N. (1994). Mef2 gene expression marks the cardiac and skeletal muscle lineages during mouse embryogenesis. *Development*, *120*(5), 1251–1263.

Edmondson, D. G., & Olson, E. N. (1989). A gene with homology to the myc similarity region of MyoD1 is expressed during myogenesis and is sufficient to activate the muscle differentiation program. *Genes & Development*, *3*(5), 628–640.

Enomoto, D., Obana, M., Miyawaki, A., Maeda, M., Nakayama, H., & Fujio, Y. (2015). Cardiac-specific ablation of the STAT3 gene in the subacute phase of myocardial infarction exacerbated cardiac remodeling. *American Journal of Physiology-Heart and Circulatory Physiology*, *309*(3), H471–H480.

Estrella, N. L., Clark, A. L., Desjardins, C. A., Nocco, S. E., & Naya, F. J. (2015). MEF2D deficiency in neonatal cardiomyocytes triggers cell cycle re-entry and programmed cell death in vitro. *Journal of Biological Chemistry*, *290*(40), 24367–24380.

Estrella, N. L., & Naya, F. J. (2014). Transcriptional networks regulating the costamere, sarcomere, and other cytoskeletal structures in striated muscle. *Cellular and Molecular Life Sciences*, *71*(9), 1641–1656.

Ewen, E. P., Snyder, C. M., Wilson, M., Desjardins, D., & Naya, F. J. (2011). The Mef2A transcription factor coordinately regulates a costamere gene program in cardiac muscle. *Journal of Biological Chemistry*, *286*(34), 29644–29653.

Fanjul-Fernández, M., Folgueras, A. R., Cabrera, S., & López-Otín, C. (2010). Matrix metalloproteinases: Evolution, gene regulation and functional analysis in mouse models. *Biochimica et Biophysica Acta (BBA) - Molecular Cell Research*, *1803*(1), 3–19. https://doi.org/10.1016/j.bbamcr.2009.07.004

Filomena, M. C., & Bang, M.-L. (2018). In the heart of the MEF2 transcription network: novel downstream effectors as potential targets for the treatment of cardiovascular disease. *Cardiovascular Research*. https://doi.org/10.1093/cvr/cvy123

Giraud, S., Bienvenu, F., Avril, S., Gascan, H., Heery, D. M., & Coqueret, O. (2002). Functional Interaction of STAT3 Transcription Factor with the Coactivator NcoA/SRC1a. *Journal of Biological Chemistry*, *277*(10), 8004–8011. https://doi.org/10.1074/jbc.m111486200

Gisselbrecht, S. S., Palagi, A., Kurland, J. V, Rogers, J. M., Ozadam, H., Zhan, Y., … Bulyk, M. L. (2020). Transcriptional Silencers in Drosophila Serve a Dual Role as Transcriptional Enhancers in Alternate Cellular Contexts. *Molecular Cell*, *77*(2), 324-337.e8. https://doi.org/10.1016/j.molcel.2019.10.004

Gittenberger-De Groot, A. C., Bartelings, M. M., Deruiter, M. C., & Poelmann, R. E. (2005). Basics of Cardiac Development for the Understanding of Congenital Heart Malformations. *Pediatric Research*, *57*(2), 169–176. https://doi.org/10.1203/01.PDR.0000148710.69159.61

Goedert, M., Cuenda, A., Craxton, M., Jakes, R., & Cohen, P. (1997). Activation of the novel stress-activated protein kinase SAPK4 by cytokines and cellular stresses is mediated by SKK3 (MKK6); comparison of its substrate specificity with that of other SAP kinases. *The EMBO Journal*, *16*(12), 3563–3571.

Gossett, L. A., Kelvin, D. J., Sternberg, E. A., & Olson, E. N. (1989). A new myocyte-specific enhancer-binding factor that recognizes a conserved element associated with multiple muscle-specific genes. *Molecular and Cellular Biology*, *9*(11), 5022–5033.

Haberland, M., Arnold, M. A., McAnally, J., Phan, D., Kim, Y., & Olson, E. N. (2007). Regulation of HDAC9 gene expression by MEF2 establishes a negative-feedback loop in the transcriptional circuitry of muscle differentiation. *Molecular and Cellular Biology*, *27*(2), 518–525.

Haberle, V., & Stark, A. (2018). Eukaryotic core promoters and the functional basis of transcription initiation. *Nature Reviews Molecular Cell Biology*, *19*(10), 621–637. https://doi.org/10.1038/s41580-018-0028-8

Haghikia, A., Ricke-Hoch, M., Stapel, B., Gorst, I., & Hilfiker-Kleiner, D. (2014). STAT3, a key regulator of cell-to-cell communication in the heart. *Cardiovascular Research*, *102*(2), 281–289.

Haghikia, A., Stapel, B., Hoch, M., & Hilfiker-Kleiner, D. (2011). STAT3 and cardiac remodeling. *Heart Failure Reviews*, *16*(1), 35–47.

Halade, G. V, Jin, Y.-F., & Lindsey, M. L. (2013). Matrix metalloproteinase (MMP)-9: A proximal biomarker for cardiac remodeling and a distal biomarker for inflammation. *Pharmacology & Therapeutics*, *139*(1), 32–40. https://doi.org/10.1016/j.pharmthera.2013.03.009

Han, A., He, J., Wu, Y., Liu, J. O., & Chen, L. (2005). Mechanism of recruitment of class II histone deacetylases by myocyte enhancer factor-2. *Journal of Molecular Biology*, *345*(1), 91–102.

Han, J., Jiang, Y., Li, Z., Kravchenko, V. V, & Ulevitch, R. J. (1997). Activation of the transcription factor MEF2C by the MAP kinase p38 in inflammation. *Nature*, *386*(6622), 296–299.

Harada, M., Qin, Y., Takano, H., Minamino, T., Zou, Y., Toko, H., … Nishi, J. (2005). G-CSF prevents cardiac remodeling after myocardial infarction by activating the Jak-Stat pathway in cardiomyocytes. *Nature Medicine*, *11*(3), 305–311.

Harhous, Z., Booz, G. W., Ovize, M., Bidaux, G., & Kurdi, M. (2019). An Update on the Multifaceted Roles of STAT3 in the Heart . *Frontiers in Cardiovascular Medicine* , Vol. 6. Retrieved from https://www.frontiersin.org/articles/10.3389/fcvm.2019.00150

Hashemi, S., Salma, J., Wales, S., & Mcdermott, J. (2015). Pro-survival function of MEF2 in cardiomyocytes is enhanced by β-blockers. *Cell Death Discovery*, *1*(1), 15019. https://doi.org/10.1038/cddiscovery.2015.19

Hashemi, S., Wales, S., Miyake, T., & Mcdermott, J. C. (2015). Heart disease: recruitment of MEF2 activity by β−blockers wards off cardiomyocyte death. *Cell Death & Disease*, *6*(10), e1916–e1916. https://doi.org/10.1038/cddis.2015.293

He, A., Kong, S. W., Ma, Q., & Pu, W. T. (2011). Co-occupancy by multiple cardiac transcription factors identifies transcriptional enhancers active in heart. *Proceedings of the National Academy of Sciences*, *108*(14), 5632–5637.

He, B. J., Joiner, M.-L. A., Singh, M. V, Luczak, E. D., Swaminathan, P. D., Koval, O. M., … Guan, X. (2011). Oxidation of CaMKII determines the cardiotoxic effects of aldosterone. *Nature Medicine*, *17*(12), 1610–1618.

Inukai, S., Kock, K. H., & Bulyk, M. L. (2017). Transcription factor–DNA binding: beyond binding site motifs. *Current Opinion in Genetics & Development*, *43*, 110–119. https://doi.org/10.1016/j.gde.2017.02.007

Itoh, M., Murata, T., Suzuki, T., Shindoh, M., Nakajima, K., Imai, K., & Yoshida, K. (2006). Requirement of STAT3 activation for maximal collagenase-1 (MMP-1) induction by epidermal growth factor and malignant characteristics in T24 bladder cancer cells. *Oncogene*, *25*(8), 1195–1204. https://doi.org/10.1038/sj.onc.1209149

Jacoby, J. J., Kalinowski, A., Liu, M.-G., Zhang, S. S.-M., Gao, Q., Chai, G.-X., … Schneider, M. (2003). Cardiomyocyte-restricted knockout of STAT3 results in higher sensitivity to inflammation, cardiac fibrosis, and heart failure with advanced age. *Proceedings of the National Academy of Sciences*, *100*(22), 12929–12934.

Jenuwein, T. (2001). Translating the Histone Code. *Science*, *293*(5532), 1074–1080. https://doi.org/10.1126/science.1063127

Jiang, J., Cai, H., Zhou, Q., & Levine, M. (1993). Conversion of a dorsal-dependent silencer into an enhancer: evidence for dorsal corepressors. *The EMBO Journal*, *12*(8), 3201–3209. https://doi.org/10.1002/j.1460-2075.1993.tb05989.x

Kataoka, Y., Matsumura, I., Ezoe, S., Nakata, S., Takigawa, E., Sato, Y., … Felsani, A. (2003). Reciprocal inhibition between MyoD and STAT3 in the regulation of growth and differentiation of myoblasts. *Journal of Biological Chemistry*, *278*(45), 44178–44187.

Kelly, D., Cockerill, G., Ng, L. L., Thompson, M., Khan, S., Samani, N. J., & Squire, I. B. (2007). Plasma matrix metalloproteinase-9 and left ventricular remodelling after acute myocardial infarction in man: a prospective cohort study. *European Heart Journal*, *28*(6), 711–718.

Kim, Y., Phan, D., Van Rooij, E., Wang, D.-Z., Mcanally, J., Qi, X., … Olson, E. N. (2008). The MEF2D transcription factor mediates stress-dependent cardiac remodeling in mice. *Journal of Clinical Investigation*, *118*(1), 124–132. https://doi.org/10.1172/jci33255

Kohli, S., Ahuja, S., & Rani, V. (2012). Transcription Factors in Heart: Promising Therapeutic Targets in Cardiac Hypertrophy. *Current Cardiology Reviews*, *7*(4), 262–271. https://doi.org/10.2174/157340311799960618

Kolovos, P., Knoch, T. A., Grosveld, F. G., Cook, P. R., & Papantonis, A. (2012). Enhancers and silencers: an integrated and simple model for their function. *Epigenetics & Chromatin*, *5*(1), 1. https://doi.org/10.1186/1756-8935-5-1

Kong, R., Bharadwaj, U., Eckols, T. K., Kolosov, M., Wu, H., Santa Cruz-Pavlovich, F. J., … Kasembeli, M. M. (2021). Novel STAT3 small-molecule inhibitors identified by structure-based virtual ligand screening incorporating SH2 domain flexibility. *Pharmacological*

Research, *169*, 105637.

Kumar, S., Jiang, M. S., Adams, J. L., & Lee, J. C. (1999). Pyridinylimidazole compound SB 203580 inhibits the activity but not the activation of p38 mitogen-activated protein kinase. *Biochemical and Biophysical Research Communications*, *263*(3), 825–831.

Kumar, S., McDonnell, P. C., Gum, R. J., Hand, A. T., Lee, J. C., & Young, P. R. (1997). Novel homologues of CSBP/p38 MAP kinase: activation, substrate specificity and sensitivity to inhibition by pyridinyl imidazoles. *Biochemical and Biophysical Research Communications*, *235*(3), 533–538.

Kurdi, M., Zgheib, C., & Booz, G. W. (2018). Recent developments on the crosstalk between STAT3 and inflammation in heart function and disease. *Frontiers in Immunology*, *9*, 3029.

Latchman, D. S. (1997). Transcription Factors: An overview. *International Journal of Biochemistry and Cell Biology*, *29*(12), 1305–1312. https://doi.org/10.1016/S1357-2725(97)00085-X

Lee, J. C., Laydon, J. T., Mcdonnell, P. C., Gallagher, T. F., Kumar, S., Green, D., … Young, P. R. (1994). A protein kinase involved in the regulation of inflammatory cytokine biosynthesis. *Nature*, *372*(6508), 739–746. https://doi.org/10.1038/372739a0

Lerner, L., Henriksen, M. A., Zhang, X., & Darnell, J. E. (2003). STAT3-dependent enhanceosome assembly and disassembly: synergy with GR for full transcriptional increase of the α2-macroglobulin gene. *Genes & Development*, *17*(20), 2564–2577. https://doi.org/10.1101/gad.1135003

Levine, M., & Tjian, R. (2003). Transcription regulation and animal diversity. *Nature*, *424*(6945), 147–151. https://doi.org/10.1038/nature01763

Li, W. X. (2008). Canonical and non-canonical JAK–STAT signaling. *Trends in Cell Biology*, *18*(11), 545–551.

Lin, Q. (1997). Control of Mouse Cardiac Morphogenesis and Myogenesis by Transcription Factor MEF2C. *Science*, *276*(5317), 1404–1407. https://doi.org/10.1126/science.276.5317.1404

Lo, S., Hsu, C., Niu, H., Niu, C., Cheng, J., & Chen, Z. (2017). Cryptotanshinone inhibits STAT3 signaling to alleviate cardiac fibrosis in type 1-like diabetic rats. *Phytotherapy Research*, *31*(4), 638–646.

Louch, W. E., Sheehan, K. A., & Wolska, B. M. (2011). Methods in cardiomyocyte isolation, culture, and gene transfer. *Journal of Molecular and Cellular Cardiology*, *51*(3), 288–298.

Lu, J., McKinsey, T. A., Nicol, R. L., & Olson, E. N. (2000). Signal-dependent activation of the MEF2 transcription factor by dissociation from histone deacetylases. *Proceedings of the National Academy of Sciences*, *97*(8), 4070–4075.

Luscombe, N. M., Austin, S. E., Berman, H. M., & Thornton, J. M. (2000). No Title. *Genome Biology*, *1*(1), reviews001.1. https://doi.org/10.1186/gb-2000-1-1-reviews001

Ma, Z., Shah, R. C., Chang, M. J., & Benveniste, E. N. (2004). Coordination of cell signaling, chromatin remodeling, histone modifications, and regulator recruitment in human matrix metalloproteinase 9 gene transcription. *Molecular and Cellular Biology*, *24*(12), 5496–

5509.

McKinsey, T. A., & Olson, E. N. (2005). Toward transcriptional therapies for the failing heart: chemical screens to modulate genes. *The Journal of Clinical Investigation*, *115*(3), 538–546.

McKinsey, T. A., Zhang, C.-L., Lu, J., & Olson, E. N. (2000). Signal-dependent nuclear export of a histone deacetylase regulates muscle differentiation. *Nature*, *408*(6808), 106–111.

Mckinsey, T. A., Zhang, C. L., & Olson, E. N. (2000). Activation of the Myocyte Enhancer Factor-2 Transcription Factor by Calcium/Calmodulin-Dependent Protein Kinase-Stimulated Binding of 14-3-3 to Histone Deacetylase 5. *Proceedings of the National Academy of Sciences*, *97*(26), 14400–14405. https://doi.org/10.1073/pnas.260501497

McKinsey, T. A., Zhang, C. L., & Olson, E. N. (2002). MEF2: a calcium-dependent regulator of cell division, differentiation and death. *Trends in Biochemical Sciences*, *27*(1), 40–47.

Medeiros, N. I., Gomes, J. A. S., Fiuza, J. A., Sousa, G. R., Almeida, E. F., Novaes, R. O., … Rocha, M. O. C. (2019). MMP-2 and MMP-9 plasma levels are potential biomarkers for indeterminate and cardiac clinical forms progression in chronic Chagas disease. *Scientific Reports*, *9*(1), 14170.

Medrano, J. L., & Naya, F. J. (2017). The transcription factor MEF2A fine-tunes gene expression in the atrial and ventricular chambers of the adult heart. *Journal of Biological Chemistry*, *292*(51), 20975–20988. https://doi.org/10.1074/jbc.m117.806422

Mika, K. M., & Lynch, V. J. (2016). An Ancient Fecundability-Associated Polymorphism Switches a Repressor into an Enhancer of Endometrial TAP2 Expression. *The American Journal of Human Genetics*, *99*(5), 1059–1071. https://doi.org/10.1016/j.ajhg.2016.09.002

Molkentin, J D, & Olson, E. N. (1996). Combinatorial control of muscle development by basic helix-loop-helix and MADS-box transcription factors. *Proceedings of the National Academy of Sciences*, *93*(18), 9366–9373. https://doi.org/10.1073/pnas.93.18.9366

Molkentin, Jeffery D, Black, B. L., Martin, J. F., & Olson, E. N. (1995). Cooperative activation of muscle gene expression by MEF2 and myogenic bHLH proteins. *Cell*, *83*(7), 1125–1136.

Morgunova, E., & Taipale, J. (2017). Structural perspective of cooperative transcription factor binding. *Current Opinion in Structural Biology*, *47*, 1–8.

Morin, S., Charron, F., Robitaille, L., & Nemer, M. (2000). GATA-dependent recruitment of MEF2 proteins to target promoters. *The EMBO Journal*, *19*(9), 2046–2055.

Moustafa, A., Hashemi, S., Brar, G., Grigull, J., Ng, S., Williams, D., … McDermott, J. (n.d.). The MEF2A Transcription Factor Interactome in Cardiomyocytes. *Cell Death & Disease*.

Nagase, H, Visse, R., & Murphy, G. (2006). Structure and function of matrix metalloproteinases and TIMPs. *Cardiovascular Research*, *69*(3), 562–573. https://doi.org/10.1016/j.cardiores.2005.12.002

Nagase, Hideaki, & Woessner, J. F. (1999). Matrix Metalloproteinases. *Journal of Biological Chemistry*, *274*(31), 21491–21494. https://doi.org/10.1074/jbc.274.31.21491

Naya, F. J., Black, B. L., Wu, H., Bassel-Duby, R., Richardson, J. A., Hill, J. A., & Olson, E. N. (2002). Mitochondrial deficiency and cardiac sudden death in mice lacking the MEF2A

transcription factor. *Nature Medicine*, *8*(11), 1303–1309. https://doi.org/10.1038/nm789

Naya, F. J., Wu, C., Richardson, J. A., Overbeek, P., & Olson, E. N. (1999). Transcriptional activity of MEF2 during mouse embryogenesis monitored with a MEF2-dependent transgene. *Development*, *126*(10), 2045–2052.

Ogbourne, S., & Antalis, T. M. (1998). Transcriptional control and the role of silencers in transcriptional regulation in eukaryotes. *Biochemical Journal*, *331*(1), 1–14. https://doi.org/10.1042/bj3310001

Olson, E. N. (2006). Gene Regulatory Networks in the Evolution and Development of the Heart. *Science*, *313*(5795), 1922–1927. https://doi.org/10.1126/science.1132292

Ornatsky, O. I., & Mcdermott, J. C. (1996). MEF2 Protein Expression, DNA Binding Specificity and Complex Composition, and Transcriptional Activity in Muscle and Non-muscle Cells. *Journal of Biological Chemistry*, *271*(40), 24927–24933. https://doi.org/10.1074/jbc.271.40.24927

Osugi, T., Oshima, Y., Fujio, Y., Funamoto, M., Yamashita, A., Negoro, S., … Hirota, H. (2002). Cardiac-specific activation of signal transducer and activator of transcription 3 promotes vascular formation in the heart. *Journal of Biological Chemistry*, *277*(8), 6676–6681.

Paige, S. L., Plonowska, K., Xu, A., & Wu, S. M. (2015). Molecular regulation of cardiomyocyte differentiation. *Circulation Research*, *116*(2), 341–353.

Paris, J., Virtanen, C., Lu, Z., & Takahashi, M. (2004). Identification of MEF2-regulated genes during muscle differentiation. *Physiological Genomics*, *20*(1), 143–151.

Parra, M., & Verdin, E. (2010). Regulatory signal transduction pathways for class IIa histone deacetylases. *Current Opinion in Pharmacology*, *10*(4), 454–460.

Patel, N. J., Nassal, D. M., Gratz, D., & Hund, T. J. (2021). Emerging therapeutic targets for cardiac arrhythmias: Role of STAT3 in regulating cardiac fibroblast function. *Expert Opinion on Therapeutic Targets*, *25*(1), 63–73.

Pereira, A. H. M., Clemente, C. F. M. Z., Cardoso, A. C., Theizen, T. H., Rocco, S. A., Judice, C. C., … Souza, J. R. M. (2009). MEF2C silencing attenuates load-induced left ventricular hypertrophy by modulating mTOR/S6K pathway in mice. *PLoS One*, *4*(12), e8472.

Perry, R. L. S., Yang, C., Soora, N., Salma, J., Marback, M., Naghibi, L., … McDermott, J. C. (2009). Direct interaction between myocyte enhancer factor 2 (MEF2) and protein phosphatase 1α represses MEF2-dependent gene expression. *Molecular and Cellular Biology*, *29*(12), 3355–3366.

Petrykowska, H. M., Vockley, C. M., & Elnitski, L. (2008). Detection and characterization of silencers and enhancer-blockers in the greater CFTR locus. *Genome Research*, *18*(8), 1238–1246. https://doi.org/10.1101/gr.073817.107

Pon, J. R., & Marra, M. A. (2016). MEF2 Transcription Factors: Developmental Regulators and Emerging Cancer Genes. *Oncotarget*, *7*(3), 2297–2312. https://doi.org/10.18632/oncotarget.6223

Prabhu, S. D., & Frangogiannis, N. G. (2016). The Biological Basis for Cardiac Repair After

Myocardial Infarction. *Circulation Research*, *119*(1), 91–112. https://doi.org/10.1161/circresaha.116.303577

Raingeaud, J., Gupta, S., Rogers, J. S., Dickens, M., Han, J., Ulevitch, R. J., & Davis, R. J. (1995). Pro-inflammatory Cytokines and Environmental Stress Cause p38 Mitogen-activated Protein Kinase Activation by Dual Phosphorylation on Tyrosine and Threonine (∗). *Journal of Biological Chemistry*, *270*(13), 7420–7426.

Sandmann, T., Jensen, L. J., Jakobsen, J. S., Karzynski, M. M., Eichenlaub, M. P., Bork, P., & Furlong, E. E. M. (2006). A temporal map of transcription factor activity: mef2 directly regulates target genes at all stages of muscle development. *Developmental Cell*, *10*(6), 797–807.

Schlesinger, J., Schueler, M., Grunert, M., Fischer, J. J., Zhang, Q., Krueger, T., … Sperling, S. R. (2011). The cardiac transcription network modulated by Gata4, Mef2a, Nkx2. 5, Srf, histone modifications, and microRNAs. *PLoS Genetics*, *7*(2), e1001313.

Sgrignani, J., Garofalo, M., Matkovic, M., Merulla, J., Catapano, C. V, & Cavalli, A. (2018). Structural biology of STAT3 and its implications for anticancer therapies development. *International Journal of Molecular Sciences*, *19*(6), 1591.

Shalizi, A., Gaudillière, B., Yuan, Z., Stegmüller, J., Shirogane, T., Ge, Q., … Bonni, A. (2006). A calcium-regulated MEF2 sumoylation switch controls postsynaptic differentiation. *Science*, *311*(5763), 1012–1017.

Song, Y., Qian, L., Song, S., Chen, L., Zhang, Y., Yuan, G., … Yu, M. (2008). Fra-1 and Stat3 synergistically regulate activation of human MMP-9 gene. *Molecular Immunology*, *45*(1), 137–143.

Soutourina, J. (2018). Transcription regulation by the Mediator complex. *Nature Reviews Molecular Cell Biology*, *19*(4), 262–274. https://doi.org/10.1038/nrm.2017.115

Spangenburg, E. E., & Booth, F. W. (2002). Multiple signaling pathways mediate LIF-induced skeletal muscle satellite cell proliferation. *American Journal of Physiology-Cell Physiology*, *283*(1), C204–C211.

Spinale, F. G. (2007). Myocardial matrix remodeling and the matrix metalloproteinases: influence on cardiac form and function. *Physiological Reviews*, *87*(4), 1285–1342.

Spitz, F., & Furlong, E. E. M. (2012). Transcription factors: From Enhancer Binding to Developmental Control. *Nature Reviews Genetics*, *13*(9), 613–626. https://doi.org/10.1038/nrg3207

Squire, I. B., Evans, J., Ng, L. L., Loftus, I. M., & Thompson, M. M. (2004). Plasma MMP-9 and MMP-2 following acute myocardial infarction in man: correlation with echocardiographic and neurohumoral parameters of left ventricular dysfunction. *Journal of Cardiac Failure*, *10*(4), 328–333. https://doi.org/10.1016/J.CARDFAIL.2003.11.003

Sun, L., Ma, K., Wang, H., Xiao, F., Gao, Y., Zhang, W., … Wu, Z. (2007). JAK1–STAT1–STAT3, a key pathway promoting proliferation and preventing premature differentiation of myoblasts. *The Journal of Cell Biology*, *179*(1), 129–138.

Takahra, T., Smart, D. E., Oakley, F., & Mann, D. A. (2004). Induction of myofibroblast MMP-9

transcription in three-dimensional collagen I gel cultures: regulation by NF-κB, AP-1 and Sp1. *The International Journal of Biochemistry & Cell Biology*, *36*(2), 353–363.

Tam, P. P. L., & Behringer, R. R. (1997). Mouse gastrulation: the formation of a mammalian body plan. *Mechanisms of Development*, *68*(1–2), 3–25.

Tang, X., Wang, X., Gong, X., Tong, M., Park, D., Xia, Z., & Mao, Z. (2005). Cyclin-dependent kinase 5 mediates neurotoxin-induced degradation of the transcription factor myocyte enhancer factor 2. *Journal of Neuroscience*, *25*(19), 4823–4834.

Tobin, S. W., Hashemi, S., Dadson, K., Turdi, S., Ebrahimian, K., Zhao, J., … Mcdermott, J. C. (2017). Heart Failure and MEF2 Transcriptome Dynamics in Response to β-Blockers. *Scientific Reports*, *7*(1). https://doi.org/10.1038/s41598-017-04762-x

Turkson, J., Bowman, T., Garcia, R., Caldenhoven, E., De Groot, R. P., & Jove, R. (1998). Stat3 Activation by Src Induces Specific Gene Regulation and Is Required for Cell Transformation. *Molecular and Cellular Biology*, *18*(5), 2545–2552. https://doi.org/10.1128/mcb.18.5.2545

Van den Steen, P. E., Dubois, B., Nelissen, I., Rudd, P. M., Dwek, R. A., & Opdenakker, G. (2002). Biochemistry and molecular biology of gelatinase B or matrix metalloproteinase-9 (MMP-9). *Critical Reviews in Biochemistry and Molecular Biology*, *37*(6), 375–536.

Van Oort, R. J., Van Rooij, E., Bourajjaj, M., Schimmel, J., Jansen, M. A., Van Der Nagel, R., … De Windt, L. J. (2006). MEF2 Activates a Genetic Program Promoting Chamber Dilation and Contractile Dysfunction in Calcineurin-Induced Heart Failure. *Circulation*, *114*(4), 298–308. https://doi.org/10.1161/circulationaha.105.608968

Verdin, E., Dequiedt, F., & Kasler, H. G. (2003). Class II Histone Deacetylases: Versatile Regulators. *Trends in Genetics*, *19*(5), 286–293. https://doi.org/10.1016/s0168-9525(03)00073-8

Vernimmen, D., & Bickmore, W. A. (2015). The Hierarchy of Transcriptional Activation: From Enhancer to Promoter. *Trends in Genetics*, *31*(12), 696–708. https://doi.org/10.1016/j.tig.2015.10.004

Vernimmen, D., Gobbi, M. De, Sloane-Stanley, J. A., Wood, W. G., & Higgs, D. R. (2007). Long-range chromosomal interactions regulate the timing of the transition between poised and active gene expression. *The EMBO Journal*, *26*(8), 2041–2051. https://doi.org/10.1038/sj.emboj.7601654

Vierstra, J., Wang, H., John, S., Sandstrom, R., & Stamatoyannopoulos, J. A. (2014). Coupling transcription factor occupancy to nucleosome architecture with DNase-FLASH. *Nature Methods*, *11*(1), 66–72. https://doi.org/10.1038/nmeth.2713

Visse, R., & Nagase, H. (2003). Matrix Metalloproteinases and Tissue Inhibitors of Metalloproteinases. *Circulation Research*, *92*(8), 827–839. https://doi.org/10.1161/01.res.0000070112.80711.3d

Vong, L. H., Ragusa, M. J., & Schwarz, J. J. (2005). Generation of conditional Mef2cloxP/loxP mice for temporal-and tissue-specific analyses. *Genesis*, *43*(1), 43–48.

Wales, S., Hashemi, S., Blais, A., & Mcdermott, J. C. (2014). Global MEF2 Target Gene

Analysis in Cardiac and Skeletal Muscle Reveals Novel Regulation of DUSP6 by p38MAPK-MEF2 Signaling. *Nucleic Acids Research*, *42*(18), 11349–11362. https://doi.org/10.1093/nar/gku813

Wang, L., Yuan, T., Du, G., Zhao, Q., Ma, L., & Zhu, J. (2014). The impact of 1, 25-dihydroxyvitamin D3 on the expression of connective tissue growth factor and transforming growth factor-β1 in the myocardium of rats with diabetes. *Diabetes Research and Clinical Practice*, *104*(2), 226–233.

Wang, X., & Khalil, R. A. (2018). Matrix metalloproteinases, vascular remodeling, and vascular disease. *Advances in Pharmacology*, *81*, 241–330.

Wang, Zhulun, Canagarajah, B. J., Boehm, J. C., Kassisà, S., Cobb, M. H., Young, P. R., … Goldsmith, E. J. (1998). Structural basis of inhibitor selectivity in MAP kinases. *Structure*, *6*(9), 1117–1128.

Wang, Zhuo, Yan, M., Li, J., Long, J., Li, Y., & Zhang, H. (2019). Dual functions of STAT3 in LPS-induced angiogenesis of hepatocellular carcinoma. *Biochimica et Biophysica Acta (BBA) - Molecular Cell Research*, *1866*(4), 566–574. https://doi.org/10.1016/J.BBAMCR.2018.11.016

Xu, J., Gong, N. L., Bodi, I., Aronow, B. J., Backx, P. H., & Molkentin, J. D. (2006). Myocyte Enhancer Factors 2A and 2C Induce Dilated Cardiomyopathy in Transgenic Mice. *Journal of Biological Chemistry*, *281*(14), 9152–9162. https://doi.org/10.1074/jbc.m510217200

Yabluchanskiy, A., Ma, Y., Iyer, R. P., Hall, M. E., & Lindsey, M. L. (2013). Matrix metalloproteinase-9: Many shades of function in cardiovascular disease. *Physiology (Bethesda, Md.)*, *28*(6), 391–403. https://doi.org/10.1152/physiol.00029.2013

Yan, C., & Boyd, D. D. (2007). Regulation of matrix metalloproteinase gene expression. *Journal of Cellular Physiology*, *211*(1), 19–26.

Yang, S.-H., Galanis, A., & Sharrocks, A. D. (1999). Targeting of p38 mitogen-activated protein kinases to MEF2 transcription factors. *Molecular and Cellular Biology*, *19*(6), 4028–4038.

Young, P. R. (2013). Perspective on the discovery and scientific impact of p38 MAP kinase. *Journal of Biomolecular Screening*, *18*(10), 1156–1163.

Young, P. R., Mclaughlin, M. M., Kumar, S., Kassis, S., Doyle, M. L., Mcnulty, D., … Lee, J. C. (1997). Pyridinyl Imidazole Inhibitors of p38 Mitogen-activated Protein Kinase Bind in the ATP Site. *Journal of Biological Chemistry*, *272*(18), 12116–12121. https://doi.org/10.1074/jbc.272.18.12116

Yu, Y. T. (1996). Distinct domains of myocyte enhancer binding factor-2A determining nuclear localization and cell type-specific transcriptional activity. *Journal of Biological Chemistry*, *271*(40), 24675–24683.

Yu, Y. T., Breitbart, R. E., Smoot, L. B., Lee, Y., Mahdavi, V., & Nadal-Ginard, B. (1992). Human myocyte-specific enhancer factor 2 comprises a group of tissue-restricted MADS box transcription factors. *Genes & Development*, *6*(9), 1783–1798. https://doi.org/10.1101/gad.6.9.1783

Zabidi, M. A., & Stark, A. (2016). Regulatory Enhancer–Core-Promoter Communication via

Transcription Factors and Cofactors. *Trends in Genetics*, *32*(12), 801–814. https://doi.org/10.1016/j.tig.2016.10.003

Zhao, M., New, L., Kravchenko, V. V, Kato, Y., Gram, H., Di Padova, F., … Han, J. (1999). Regulation of the MEF2 family of transcription factors by p38. *Molecular and Cellular Biology*, *19*(1), 21–30.

Zhao, X., Nozell, S., Ma, Z., & Benveniste, E. N. (2007). The interferon-stimulated gene factor 3 complex mediates the inhibitory effect of interferon-β on matrix metalloproteinase-9 expression. *The FEBS Journal*, *274*(24), 6456–6468.

Zouein, F. A., Kurdi, M., & Booz, G. W. (2013). Dancing rhinos in stilettos: the amazing saga of the genomic and nongenomic actions of STAT3 in the heart. *Jak-Stat*, *2*(3), e24352.

Zugowski, C., Lieder, F., Müller, A., Gasch, J., Corvinus, F. M., Moriggl, R., & Friedrich, K. (2011). *STAT3 controls matrix metalloproteinase-1 expression in colon carcinoma cells by both direct and AP-1-mediated interaction with the MMP-1 promoter*. *392*(5), 449–459. https://doi.org/doi:10.1515/bc.2011.038

APPENDIX A

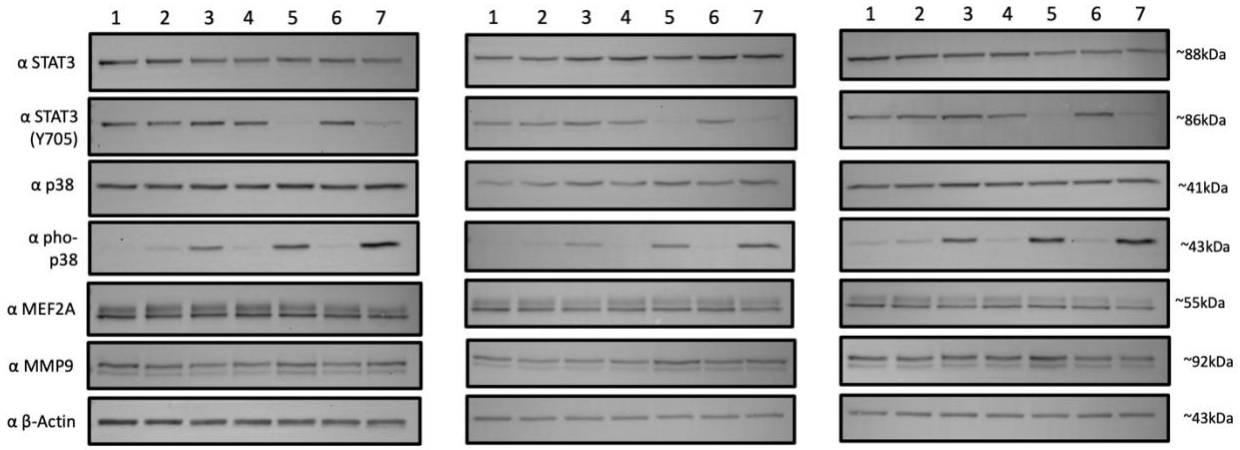

Figure A1: Independent western blot trials for pharmacological inhibition treatments in NRVMs.

Lane 1: Untreated; Lane 2: SB202470, Lane 3: SB203580, Lane 4: DMSO, Lane 5: C188-9, Lane 6: SB202470 and DMSO, Lane 7: SB203580 and C188-9.

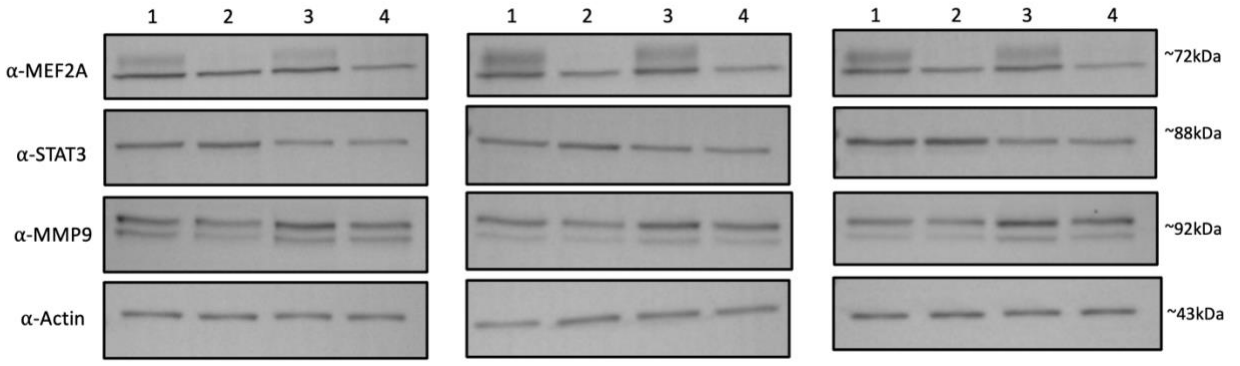

Figure A2: Independent western blot trials of si-RNA mediated gene silencing in NRVMs.

Lane 1: Scrambled control siRNA; Lane 2: siMEF2A#1, Lane 3: siSTAT3#1, Lane 4: siMEF2A#1 and siSTAT3#1